Supporting Information

A Family of $Co^{II}Co^{III}_3$ Single-Ion Magnets with Zero-Field Slow Magnetic Relaxation: Fine Tuning of Energy Barrier by Remote Substituent and Counter Cation

Yuan-Yuan Zhu,[†,‡] Yi-Quan Zhang,[‡,§] Ting-Ting Yin,[†] Chen Gao,[‡] Bing-Wu Wang,[‡] and Song Gao*[‡]*

[†]*School of Chemistry and Chemical Engineering, Hefei University of Technology and Anhui Key Laboratory of Advanced Functional Materials and Devices, Hefei 230009, China*

[‡]*Beijing National Laboratory for Molecular Sciences, State Key Laboratory of Rare Earth Materials Chemistry and Applications, College of Chemistry and Molecular Engineering, Peking University, Beijing 100871, China*

[§]*Jiangsu Key Laboratory for NSLSCS, School of Physical Science and Technology, Nanjing Normal University, Nanjing 210023, China*

Corresponding Author E-mail address: yyzhu@hfut.edu.cn; gaosong@pku.edu.cn

Table S1. Selected bond lengths (Å) and angles (°) for **2*R***.

Co(1)-O(2)	2.151(4)	Co(1)-O(2)#1	2.151(4)
Co(1)-O(2)#2	2.151(4)	Co(1)-O(4)	2.155(4)
Co(1)-O(4)#1	2.155(4)	Co(1)-O(4)#2	2.155(4)
Co(2)-O(1)	1.931(5)	Co(2)-O(2)	1.896(4)
Co(2)-O(3)	1.895(4)	Co(2)-O(4)	1.893(4)
Co(2)-N(1)	1.918(5)	Co(2)-N(2)	1.912(5)
O(2)#1-Co(1)-O(2)#2	90.86(16)	O(2)#1-Co(1)-O(2)	90.86(16)
O(2)#2-Co(1)-O(2)	90.86(16)	O(2)#1-Co(1)-O(4)	115.74(14)
O(2)#2-Co(1)-O(4)	147.67(15)	O(2)-Co(1)-O(4)	71.75(15)
O(2)#1-Co(1)-O(4)#2	147.67(15)	O(2)#2-Co(1)-O(4)#2	71.75(15)
O(2)-Co(1)-O(4)#2	115.74(14)	O(4)-Co(1)-O(4)#2	91.08(15)

O(2)#1-Co(1)-O(4)#1	71.75(15)	O(2)#2-Co(1)-O(4)#1	115.74(14)
O(2)-Co(1)-O(4)#1	147.67(15)	O(4)-Co(1)-O(4)#1	91.08(15)
O(4)#2-Co(1)-O(4)#1	91.08(15)	O(4)-Co(2)-O(3)	92.92(19)
O(4)-Co(2)-O(2)	83.51(17)	O(3)-Co(2)-O(2)	175.50(19)
O(4)-Co(2)-N(2)	95.3(2)	O(3)-Co(2)-N(2)	93.1(2)
O(2)-Co(2)-N(2)	84.6(2)	O(4)-Co(2)-N(1)	84.44(18)
O(3)-Co(2)-N(1)	87.8(2)	O(2)-Co(2)-N(1)	94.54(19)
N(2)-Co(2)-N(1)	179.1(2)	O(4)-Co(2)-O(1)	176.0(2)
O(3)-Co(2)-O(1)	90.3(2)	O(2)-Co(2)-O(1)	93.3(2)
N(2)-Co(2)-O(1)	86.9(2)	N(1)-Co(2)-O(1)	93.3(2)

[a] Symmetry operation: #1, -z+1/2,-x,y+1/2; #2, -y,z-1/2,-x+1/2.

Table S2. Selected bond lengths (Å) and angles (°) for **2*S***.

Co(1)-O(2)	2.142(5)	Co(1)-O(2)#1	2.142(5)
Co(1)-O(2)#2	2.142(5)	Co(1)-O(4)	2.161(5)
Co(1)-O(4)#1	2.161(5)	Co(1)-O(4)#2	2.161(5)
Co(2)-O(1)	1.905(6)	Co(2)-O(2)	1.900(5)
Co(2)-O(3)	1.914(5)	Co(2)-O(4)	1.890(5)
Co(2)-N(1)	1.908(5)	Co(2)-N(2)	1.917(6)
O(2)-Co(1)-O(2)#1	91.28(18)	O(2)-Co(1)-O(2)#2	91.28(18)
O(2)#1-Co(1)-O(2)#2	91.28(18)	O(2)-Co(1)-O(4)#2	114.83(17)
O(2)#1-Co(1)-O(4)#2	148.39(19)	O(2)#2-Co(1)-O(4)#2	71.64(18)
O(2)-Co(1)-O(4)	71.64(18)	O(2)#1-Co(1)-O(4)	114.83(17)
O(2)#2-Co(1)-O(4)	148.39(19)	O(4)#2-Co(1)-O(4)	91.21(18)
O(2)-Co(1)-O(4)#1	148.39(18)	O(2)#1-Co(1)-O(4)#1	71.64(18)
O(2)#2-Co(1)-O(4)#1	114.83(18)	O(4)#2-Co(1)-O(4)#1	91.21(18)
O(4)-Co(1)-O(4)#1	91.21(18)	O(4)-Co(2)-O(2)	83.3(2)
O(4)-Co(2)-O(1)	93.0(2)	O(2)-Co(2)-O(1)	175.4(2)
O(4)-Co(2)-N(1)	94.0(2)	O(2)-Co(2)-N(1)	84.0(2)
O(1)-Co(2)-N(1)	93.6(2)	O(4)-Co(2)-O(3)	176.2(2)
O(2)-Co(2)-O(3)	93.6(2)	O(1)-Co(2)-O(3)	90.2(2)
N(1)-Co(2)-O(3)	87.9(2)	O(4)-Co(2)-N(2)	84.6(2)
O(2)-Co(2)-N(2)	94.6(2)	O(1)-Co(2)-N(2)	87.7(3)
N(1)-Co(2)-N(2)	178.1(3)	O(3)-Co(2)-N(2)	93.5(2)

[a] Symmetry operation: #1, -y+1,z-1/2,-x+3/2; #2, -z+3/2,-x+1,y+1/2.

Table S3. Selected bond lengths (Å) and angles (°) for **3*S***.

Co(1)-O(6)	2.134(3)	Co(3)-N(3)	1.891(4)
Co(1)-O(4)	2.137(3)	Co(3)-O(8)	1.900(3)
Co(1)-O(12)	2.139(3)	Co(3)-N(4)	1.900(4)
Co(1)-O(2)	2.156(3)	Co(3)-O(5)	1.905(3)
Co(1)-O(10)	2.169(3)	Co(3)-O(6)	1.906(3)
Co(1)-O(8)	2.169(3)	Co(3)-O(7)	1.921(3)
Co(2)-O(2)	1.899(3)	Co(4)-O(12)	1.899(3)
Co(2)-N(2)	1.903(4)	Co(4)-O(10)	1.902(3)
Co(2)-O(1)	1.908(3)	Co(4)-N(5)	1.906(4)
Co(2)-N(1)	1.913(4)	Co(4)-O(9)	1.913(3)
Co(2)-O(3)	1.915(3)	Co(4)-N(6)	1.918(4)
Co(2)-O(4)	1.916(3)	Co(4)-O(11)	1.920(3)
O(6)-Co(1)-O(4)	147.97(12)	N(3)-Co(3)-O(8)	95.23(15)
O(6)-Co(1)-O(12)	116.07(12)	N(3)-Co(3)-N(4)	178.02(16)
O(4)-Co(1)-O(12)	90.95(12)	O(8)-Co(3)-N(4)	83.57(15)
O(6)-Co(1)-O(2)	89.21(12)	N(3)-Co(3)-O(5)	93.98(15)
O(4)-Co(1)-O(2)	72.35(12)	O(8)-Co(3)-O(5)	92.88(14)
O(12)-Co(1)-O(2)	149.14(12)	N(4)-Co(3)-O(5)	87.66(15)
O(6)-Co(1)-O(10)	93.16(12)	N(3)-Co(3)-O(6)	84.58(14)
O(4)-Co(1)-O(10)	112.58(12)	O(8)-Co(3)-O(6)	84.00(13)
O(12)-Co(1)-O(10)	71.39(12)	N(4)-Co(3)-O(6)	93.72(14)
O(2)-Co(1)-O(10)	90.87(12)	O(5)-Co(3)-O(6)	176.41(14)
O(6)-Co(1)-O(8)	72.58(12)	N(3)-Co(3)-O(7)	87.24(15)
O(4)-Co(1)-O(8)	92.35(12)	O(8)-Co(3)-O(7)	175.98(14)
O(12)-Co(1)-O(8)	88.72(12)	N(4)-Co(3)-O(7)	93.87(16)
O(2)-Co(1)-O(8)	117.02(12)	O(5)-Co(3)-O(7)	90.12(14)
O(10)-Co(1)-O(8)	147.70(12)	O(6)-Co(3)-O(7)	93.09(13)
O(2)-Co(2)-N(2)	92.89(14)	O(12)-Co(4)-O(10)	82.79(13)
O(2)-Co(2)-O(1)	175.48(14)	O(12)-Co(4)-N(5)	95.57(15)
N(2)-Co(2)-O(1)	88.89(15)	O(10)-Co(4)-N(5)	84.10(15)
O(2)-Co(2)-N(1)	84.02(15)	O(12)-Co(4)-O(9)	92.59(14)
N(2)-Co(2)-N(1)	176.90(16)	O(10)-Co(4)-O(9)	174.77(14)
O(1)-Co(2)-N(1)	94.21(15)	N(5)-Co(4)-O(9)	93.95(15)
O(2)-Co(2)-O(3)	93.75(14)	O(12)-Co(4)-N(6)	84.30(14)
N(2)-Co(2)-O(3)	94.06(15)	O(10)-Co(4)-N(6)	94.13(15)
O(1)-Co(2)-O(3)	90.27(15)	N(5)-Co(4)-N(6)	178.23(17)
N(1)-Co(2)-O(3)	85.90(15)	O(9)-Co(4)-N(6)	87.82(15)
O(2)-Co(2)-O(4)	83.27(14)	O(12)-Co(4)-O(11)	175.80(15)
N(2)-Co(2)-O(4)	83.69(15)	O(10)-Co(4)-O(11)	94.16(14)
O(1)-Co(2)-O(4)	92.80(14)	N(5)-Co(4)-O(11)	86.95(15)
N(1)-Co(2)-O(4)	96.17(15)	O(9)-Co(4)-O(11)	90.57(15)
O(3)-Co(2)-O(4)	176.16(14)	N(6)-Co(4)-O(11)	93.07(15)

Table S4. Selected bond lengths (Å) and angles (°) for **4*R***.

Co(1)-O(2)	2.058(3)	Co(1)-O(4)	2.335(3)
Co(1)-O(6)	2.129(3)	Co(1)-O(8)	2.115(3)
Co(1)-O(10)	2.294(3)	Co(1)-O(12)	2.068(3)
Co(2)-O(1)	1.893(3)	Co(2)-O(2)	1.902(3)
Co(2)-O(3)	1.917(3)	Co(2)-O(4)	1.884(3)
Co(2)-N(1)	1.902(3)	Co(2)-N(2)	1.903(3)
Co(3)-O(5)	1.898(3)	Co(3)-O(6)	1.895(3)
Co(3)-O(7)	1.899(3)	Co(3)-O(8)	1.907(3)
Co(3)-N(3)	1.900(3)	Co(3)-N(4)	1.892(3)
Co(4)-O(9)	1.915(3)	Co(4)-O(10)	1.890(2)
Co(4)-O(11)	1.902(2)	Co(4)-O(12)	1.913(2)
Co(4)-N(5)	1.906(3)	Co(4)-N(6)	1.895(3)
O(2)-Co(1)-O(12)	145.27(10)	O(2)-Co(1)-O(8)	112.49(10)
O(12)-Co(1)-O(8)	95.97(10)	O(2)-Co(1)-O(6)	96.86(10)
O(12)-Co(1)-O(6)	111.28(10)	O(8)-Co(1)-O(6)	71.47(9)
O(2)-Co(1)-O(10)	90.33(9)	O(12)-Co(1)-O(10)	70.51(9)
O(8)-Co(1)-O(10)	151.58(10)	O(6)-Co(1)-O(10)	89.83(9)
O(2)-Co(1)-O(4)	70.36(9)	O(12)-Co(1)-O(4)	91.43(10)
O(8)-Co(1)-O(4)	89.20(10)	O(6)-Co(1)-O(4)	151.12(9)
O(10)-Co(1)-O(4)	115.27(9)	O(4)-Co(2)-O(1)	94.81(12)
O(4)-Co(2)-O(2)	84.31(11)	O(1)-Co(2)-O(2)	178.85(11)
O(4)-Co(2)-N(1)	93.54(12)	O(1)-Co(2)-N(1)	94.52(13)
O(2)-Co(2)-N(1)	84.80(13)	O(4)-Co(2)-N(2)	83.95(12)
O(1)-Co(2)-N(2)	86.52(12)	O(2)-Co(2)-N(2)	94.12(12)
N(1)-Co(2)-N(2)	177.35(14)	O(4)-Co(2)-O(3)	175.76(12)
O(1)-Co(2)-O(3)	88.54(11)	O(2)-Co(2)-O(3)	92.37(11)
N(1)-Co(2)-O(3)	88.78(12)	N(2)-Co(2)-O(3)	93.68(12)
N(4)-Co(3)-O(6)	94.17(12)	N(4)-Co(3)-O(5)	86.51(13)
O(6)-Co(3)-O(5)	175.52(12)	N(4)-Co(3)-O(7)	94.42(13)
O(6)-Co(3)-O(7)	94.66(12)	O(5)-Co(3)-O(7)	89.70(12)
N(4)-Co(3)-N(3)	178.65(14)	O(6)-Co(3)-N(3)	84.71(12)
O(5)-Co(3)-N(3)	94.67(13)	O(7)-Co(3)-N(3)	84.93(12)
N(4)-Co(3)-O(8)	83.15(13)	O(6)-Co(3)-O(8)	81.37(11)
O(5)-Co(3)-O(8)	94.33(12)	O(7)-Co(3)-O(8)	175.15(12)
N(3)-Co(3)-O(8)	97.41(12)	O(10)-Co(4)-N(6)	93.48(12)
O(10)-Co(4)-O(11)	94.14(11)	N(6)-Co(4)-O(11)	94.06(12)
O(10)-Co(4)-N(5)	84.63(12)	N(6)-Co(4)-N(5)	177.89(14)
O(11)-Co(4)-N(5)	85.16(12)	O(10)-Co(4)-O(12)	83.16(10)
N(6)-Co(4)-O(12)	84.66(12)	O(11)-Co(4)-O(12)	176.93(12)
N(5)-Co(4)-O(12)	96.02(12)	O(10)-Co(4)-O(9)	175.33(12)
N(6)-Co(4)-O(9)	87.65(12)	O(11)-Co(4)-O(9)	90.30(10)

N(5)-Co(4)-O(9)	94.31(13)	O(12)-Co(4)-O(9)	92.43(11)

Table S5. Selected bond lengths (Å) and angles (°) for **5*R***.

Co(1)-O(2)	2.122(7)	Co(3)-O(5)	1.889(7)
Co(1)-O(6)	2.137(7)	Co(3)-O(7)	1.890(7)
Co(1)-O(12)	2.143(7)	Co(3)-O(6)	1.899(7)
Co(1)-O(8)	2.164(7)	Co(3)-O(8)	1.908(7)
Co(1)-O(10)	2.174(7)	Co(3)-N(4)	1.918(9)
Co(1)-O(4)	2.178(7)	Co(3)-N(3)	1.921(8)
Co(2)-O(1)	1.884(7)	Co(4)-O(10)	1.896(7)
Co(2)-O(4)	1.886(7)	Co(4)-O(9)	1.898(7)
Co(2)-N(2)	1.900(8)	Co(4)-O(12)	1.900(6)
Co(2)-O(3)	1.901(7)	Co(4)-N(6)	1.900(8)
Co(2)-O(2)	1.902(7)	Co(4)-N(5)	1.909(9)
Co(2)-N(1)	1.912(8)	Co(4)-O(11)	1.910(7)
O(2)-Co(1)-O(6)	90.2(3)	O(5)-Co(3)-O(7)	90.8(3)
O(2)-Co(1)-O(12)	144.9(3)	O(5)-Co(3)-O(6)	176.0(3)
O(6)-Co(1)-O(12)	119.4(3)	O(7)-Co(3)-O(6)	93.1(3)
O(2)-Co(1)-O(8)	117.6(3)	O(5)-Co(3)-O(8)	93.4(3)
O(6)-Co(1)-O(8)	71.6(3)	O(7)-Co(3)-O(8)	175.8(3)
O(12)-Co(1)-O(8)	91.2(3)	O(6)-Co(3)-O(8)	82.7(3)
O(2)-Co(1)-O(10)	91.6(3)	O(5)-Co(3)-N(4)	86.4(3)
O(6)-Co(1)-O(10)	89.5(3)	O(7)-Co(3)-N(4)	95.0(3)
O(12)-Co(1)-O(10)	71.7(2)	O(6)-Co(3)-N(4)	94.3(3)
O(8)-Co(1)-O(10)	144.4(3)	O(8)-Co(3)-N(4)	84.6(3)
O(2)-Co(1)-O(4)	71.9(3)	O(5)-Co(3)-N(3)	93.5(3)
O(6)-Co(1)-O(4)	144.8(3)	O(7)-Co(3)-N(3)	85.2(3)
O(12)-Co(1)-O(4)	89.7(3)	O(6)-Co(3)-N(3)	85.9(3)
O(8)-Co(1)-O(4)	89.8(3)	O(8)-Co(3)-N(3)	95.3(3)
O(10)-Co(1)-O(4)	120.1(3)	N(4)-Co(3)-N(3)	179.8(4)
O(1)-Co(2)-O(4)	93.4(3)	O(10)-Co(4)-O(9)	175.8(3)
O(1)-Co(2)-N(2)	85.3(3)	O(10)-Co(4)-O(12)	83.5(3)
O(4)-Co(2)-N(2)	85.1(3)	O(9)-Co(4)-O(12)	92.3(3)
O(1)-Co(2)-O(3)	91.4(3)	O(10)-Co(4)-N(6)	94.2(3)
O(4)-Co(2)-O(3)	175.0(3)	O(9)-Co(4)-N(6)	86.1(3)
N(2)-Co(2)-O(3)	94.1(3)	O(12)-Co(4)-N(6)	83.8(3)
O(1)-Co(2)-O(2)	176.4(3)	O(10)-Co(4)-N(5)	85.8(3)
O(4)-Co(2)-O(2)	83.6(3)	O(9)-Co(4)-N(5)	94.0(3)
N(2)-Co(2)-O(2)	96.3(3)	O(12)-Co(4)-N(5)	96.7(3)
O(3)-Co(2)-O(2)	91.6(3)	N(6)-Co(4)-N(5)	179.5(4)
O(1)-Co(2)-N(1)	93.8(3)	O(10)-Co(4)-O(11)	93.1(3)
O(4)-Co(2)-N(1)	94.1(3)	O(9)-Co(4)-O(11)	91.1(3)

N(2)-Co(2)-N(1)	178.7(4)	O(12)-Co(4)-O(11)	176.0(3)
O(3)-Co(2)-N(1)	86.8(3)	N(6)-Co(4)-O(11)	94.4(3)
O(2)-Co(2)-N(1)	84.5(3)	N(5)-Co(4)-O(11)	85.1(3)

Table S6. Selected bond lengths (Å) and angles (°) for **6*R***.

Co(1)-O(14)	2.105(2)	Co(3)-O(10)	1.8976(19)
Co(1)-O(2)	2.1294(19)	Co(3)-O(14)	1.9004(18)
Co(1)-O(18)	2.137(2)	Co(3)-O(9)	1.9064(19)
Co(1)-O(22)	2.150(2)	Co(3)-N(4)	1.906(2)
Co(1)-O(6)	2.161(2)	Co(3)-O(13)	1.9092(18)
Co(1)-O(10)	2.1664(19)	Co(3)-N(3)	1.916(2)
Co(2)-O(6)	1.8955(19)	Co(4)-O(22)	1.8991(19)
Co(2)-O(2)	1.9030(18)	Co(4)-O(18)	1.9035(19)
Co(2)-O(5)	1.905(2)	Co(4)-O(17)	1.9078(19)
Co(2)-O(1)	1.9084(19)	Co(4)-N(5)	1.911(2)
Co(2)-N(2)	1.911(2)	Co(4)-O(21)	1.911(2)
Co(2)-N(1)	1.912(2)	Co(4)-N(6)	1.917(2)
O(14)-Co(1)-O(2)	117.42(8)	O(10)-Co(3)-O(14)	82.54(8)
O(14)-Co(1)-O(18)	144.35(8)	O(10)-Co(3)-O(9)	174.97(8)
O(2)-Co(1)-O(18)	92.08(8)	O(14)-Co(3)-O(9)	92.56(8)
O(14)-Co(1)-O(22)	91.10(7)	O(10)-Co(3)-N(4)	96.03(9)
O(2)-Co(1)-O(22)	144.44(7)	O(14)-Co(3)-N(4)	85.01(9)
O(18)-Co(1)-O(22)	71.90(7)	O(9)-Co(3)-N(4)	84.61(9)
O(14)-Co(1)-O(6)	91.35(7)	O(10)-Co(3)-O(13)	93.91(8)
O(2)-Co(1)-O(6)	71.49(7)	O(14)-Co(3)-O(13)	176.38(9)
O(18)-Co(1)-O(6)	118.24(7)	O(9)-Co(3)-O(13)	91.00(9)
O(22)-Co(1)-O(6)	88.10(7)	N(4)-Co(3)-O(13)	94.68(9)
O(14)-Co(1)-O(10)	71.80(7)	O(10)-Co(3)-N(3)	84.59(9)
O(2)-Co(1)-O(10)	89.22(7)	O(14)-Co(3)-N(3)	95.33(9)
O(18)-Co(1)-O(10)	90.29(7)	O(9)-Co(3)-N(3)	94.79(9)
O(22)-Co(1)-O(10)	121.42(7)	N(4)-Co(3)-N(3)	179.33(11)
O(6)-Co(1)-O(10)	145.24(7)	O(13)-Co(3)-N(3)	85.02(9)
O(6)-Co(2)-O(2)	82.57(8)	O(22)-Co(4)-O(18)	82.89(8)
O(6)-Co(2)-O(5)	175.83(9)	O(22)-Co(4)-O(17)	91.92(9)
O(2)-Co(2)-O(5)	93.41(9)	O(18)-Co(4)-O(17)	174.71(9)
O(6)-Co(2)-O(1)	93.76(9)	O(22)-Co(4)-N(5)	95.90(9)
O(2)-Co(2)-O(1)	176.25(9)	O(18)-Co(4)-N(5)	84.75(9)
O(5)-Co(2)-O(1)	90.28(9)	O(17)-Co(4)-N(5)	94.84(9)
O(6)-Co(2)-N(2)	84.55(9)	O(22)-Co(4)-O(21)	175.91(9)
O(2)-Co(2)-N(2)	94.29(9)	O(18)-Co(4)-O(21)	93.17(9)
O(5)-Co(2)-N(2)	94.66(9)	O(17)-Co(4)-O(21)	92.04(9)
O(1)-Co(2)-N(2)	86.05(9)	N(5)-Co(4)-O(21)	84.77(9)

O(6)-Co(2)-N(1)	95.31(9)	O(22)-Co(4)-N(6)	85.09(9)
O(2)-Co(2)-N(1)	84.97(9)	O(18)-Co(4)-N(6)	95.96(9)
O(5)-Co(2)-N(1)	85.43(10)	O(17)-Co(4)-N(6)	84.53(9)
O(1)-Co(2)-N(1)	94.68(9)	N(5)-Co(4)-N(6)	178.84(10)
N(2)-Co(2)-N(1)	179.27(10)	O(21)-Co(4)-N(6)	94.28(9)

Table S7. Selected bond lengths (Å) and angles (°) for **7*R***.

Co(1)-O(8)	2.1258(17)	Co(2)-N(1)	1.8976(19)
Co(1)-O(8)#1	2.1258(17)	Co(2)-O(1)	1.9109(19)
Co(1)-O(12)#1	2.1355(17)	Co(2)-O(1)#1	1.9109(19)
Co(1)-O(12)	2.1355(17)	Co(3)-O(12)	1.8877(18)
Co(1)-O(4)#1	2.1415(17)	Co(3)-O(8)	1.8949(16)
Co(1)-O(4)	2.1415(17)	Co(3)-N(5)	1.899(2)
Co(2)-O(4)#1	1.8919(18)	Co(3)-O(5)	1.9001(18)
Co(2)-O(4)	1.8919(18)	Co(3)-O(9)	1.9049(18)
Co(2)-N(1)#1	1.8976(19)	Co(3)-N(3)	1.916(2)
O(8)-Co(1)-O(8)#1	117.69(10)	N(1)#1-Co(2)-O(1)	87.51(8)
O(8)-Co(1)-O(12)#1	90.16(6)	N(1)-Co(2)-O(1)	93.89(8)
O(8)#1-Co(1)-O(12)#1	72.10(6)	O(4)#1-Co(2)-O(1)#1	177.22(8)
O(8)-Co(1)-O(12)	72.10(6)	O(4)-Co(2)-O(1)#1	93.33(8)
O(8)#1-Co(1)-O(12)	90.16(6)	N(1)#1-Co(2)-O(1)#1	93.89(8)
O(12)#1-Co(1)-O(12)	145.78(10)	N(1)-Co(2)-O(1)#1	87.51(8)
O(8)-Co(1)-O(4)#1	90.51(7)	O(1)-Co(2)-O(1)#1	89.09(13)
O(8)#1-Co(1)-O(4)#1	145.52(6)	O(12)-Co(3)-O(8)	83.06(7)
O(12)#1-Co(1)-O(4)#1	89.56(6)	O(12)-Co(3)-N(5)	84.55(8)
O(12)-Co(1)-O(4)#1	118.79(6)	O(8)-Co(3)-N(5)	94.73(8)
O(8)-Co(1)-O(4)	145.52(6)	O(12)-Co(3)-O(5)	92.65(8)
O(8)#1-Co(1)-O(4)	90.51(7)	O(8)-Co(3)-O(5)	175.35(8)
O(12)#1-Co(1)-O(4)	118.79(6)	N(5)-Co(3)-O(5)	86.61(9)
O(12)-Co(1)-O(4)	89.56(6)	O(12)-Co(3)-O(9)	177.65(8)
O(4)#1-Co(1)-O(4)	72.71(9)	O(8)-Co(3)-O(9)	94.91(8)
O(4)#1-Co(2)-O(4)	84.29(10)	N(5)-Co(3)-O(9)	94.45(9)
O(4)#1-Co(2)-N(1)#1	84.86(8)	O(5)-Co(3)-O(9)	89.41(8)
O(4)-Co(2)-N(1)#1	93.68(8)	O(12)-Co(3)-N(3)	95.22(8)
O(4)#1-Co(2)-N(1)	93.68(8)	O(8)-Co(3)-N(3)	84.14(8)
O(4)-Co(2)-N(1)	84.86(8)	N(5)-Co(3)-N(3)	178.87(9)
N(1)#1-Co(2)-N(1)	178.03(13)	O(5)-Co(3)-N(3)	94.50(9)
O(4)#1-Co(2)-O(1)	93.33(8)	O(9)-Co(3)-N(3)	85.74(9)
O(4)-Co(2)-O(1)	177.22(8)		

[a] Symmetry operation: #1 y, x, -z

Table S8. Selected bond lengths (Å) and angles (°) for **8*R***.

Co(1)-O(14)	2.129(3)	Co(3)-N(7)	1.897(3)
Co(1)-O(18)	2.134(3)	Co(3)-O(14)	1.899(3)
Co(1)-O(2)	2.143(3)	Co(3)-N(5)	1.904(3)
Co(1)-O(22)	2.147(3)	Co(3)-O(9)	1.905(3)
Co(1)-O(10)	2.150(2)	Co(3)-O(10)	1.906(3)
Co(1)-O(6)	2.154(2)	Co(3)-O(13)	1.907(3)
Co(2)-O(6)	1.886(3)	Co(4)-O(22)	1.886(3)
Co(2)-O(5)	1.897(3)	Co(4)-O(17)	1.893(3)
Co(2)-O(2)	1.899(2)	Co(4)-O(18)	1.895(3)
Co(2)-O(1)	1.906(3)	Co(4)-N(11)	1.903(3)
Co(2)-N(1)	1.912(3)	Co(4)-O(21)	1.903(3)
Co(2)-N(3)	1.922(3)	Co(4)-N(9)	1.921(3)
O(14)-Co(1)-O(18)	119.62(10)	N(7)-Co(3)-O(14)	84.90(12)
O(14)-Co(1)-O(2)	146.40(10)	N(7)-Co(3)-N(5)	178.66(13)
O(18)-Co(1)-O(2)	88.90(10)	O(14)-Co(3)-N(5)	94.30(12)
O(14)-Co(1)-O(22)	89.50(10)	N(7)-Co(3)-O(9)	87.03(12)
O(18)-Co(1)-O(22)	72.10(10)	O(14)-Co(3)-O(9)	91.86(11)
O(2)-Co(1)-O(22)	117.91(10)	N(5)-Co(3)-O(9)	94.08(12)
O(14)-Co(1)-O(10)	73.22(10)	N(7)-Co(3)-O(10)	94.74(12)
O(18)-Co(1)-O(10)	90.76(10)	O(14)-Co(3)-O(10)	84.21(11)
O(2)-Co(1)-O(10)	90.27(10)	N(5)-Co(3)-O(10)	84.10(12)
O(22)-Co(1)-O(10)	145.79(9)	O(9)-Co(3)-O(10)	175.52(12)
O(14)-Co(1)-O(6)	91.42(10)	N(7)-Co(3)-O(13)	93.85(12)
O(18)-Co(1)-O(6)	142.45(10)	O(14)-Co(3)-O(13)	176.60(12)
O(2)-Co(1)-O(6)	71.46(10)	N(5)-Co(3)-O(13)	86.88(12)
O(22)-Co(1)-O(6)	88.89(9)	O(9)-Co(3)-O(13)	91.23(12)
O(10)-Co(1)-O(6)	120.08(10)	O(10)-Co(3)-O(13)	92.75(12)
O(6)-Co(2)-O(5)	175.05(12)	O(22)-Co(4)-O(17)	92.50(12)
O(6)-Co(2)-O(2)	83.06(11)	O(22)-Co(4)-O(18)	83.55(11)
O(5)-Co(2)-O(2)	92.16(11)	O(17)-Co(4)-O(18)	175.72(11)
O(6)-Co(2)-O(1)	93.42(11)	O(22)-Co(4)-N(11)	84.57(12)
O(5)-Co(2)-O(1)	91.39(12)	O(17)-Co(4)-N(11)	86.04(12)
O(2)-Co(2)-O(1)	176.30(12)	O(18)-Co(4)-N(11)	95.20(12)
O(6)-Co(2)-N(1)	95.52(12)	O(22)-Co(4)-O(21)	176.76(12)
O(5)-Co(2)-N(1)	85.31(12)	O(17)-Co(4)-O(21)	90.44(12)
O(2)-Co(2)-N(1)	85.17(12)	O(18)-Co(4)-O(21)	93.56(11)
O(1)-Co(2)-N(1)	94.09(12)	N(11)-Co(4)-O(21)	94.26(12)
O(6)-Co(2)-N(3)	84.98(12)	O(22)-Co(4)-N(9)	96.16(12)
O(5)-Co(2)-N(3)	94.31(12)	O(17)-Co(4)-N(9)	93.65(12)
O(2)-Co(2)-N(3)	96.28(12)	O(18)-Co(4)-N(9)	85.17(12)
O(1)-Co(2)-N(3)	84.48(12)	N(11)-Co(4)-N(9)	179.21(13)
N(1)-Co(2)-N(3)	178.51(12)	O(21)-Co(4)-N(9)	85.02(12)

The magnetic data of compound 2*R* and **2*S***.

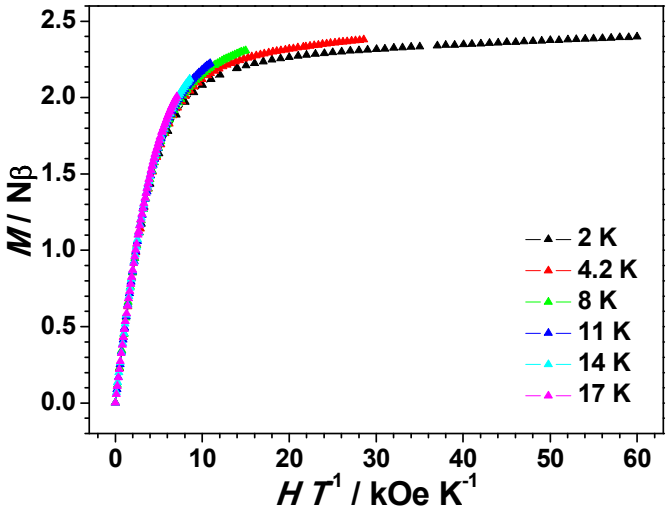

Figure S1. *M vs*. *H*/*T* plots of **2*R*** at different temperatures (2 K, 4.2 K, 8 K, 11 K, 14 K, and 17 K). It is found that the bifurcation of curves is significant at high field range.

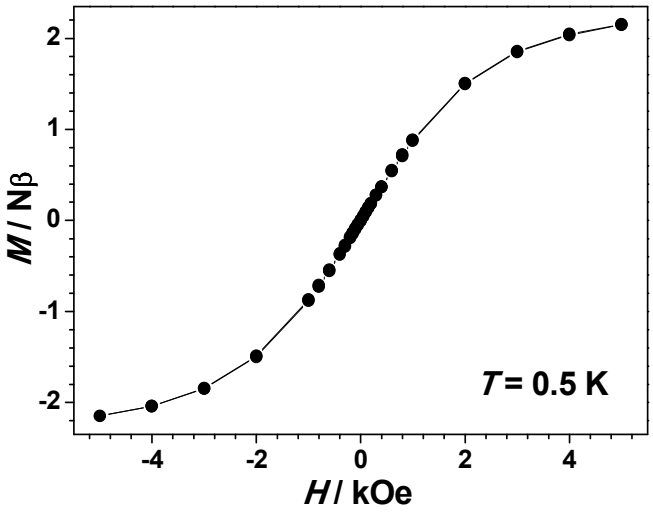

Figure S2. Magnetization *vs*. field measured for the **2*R*** at 0.5 K from -5 kOe to 5 kOe in MPMS, no hysteresis loop can be observed.

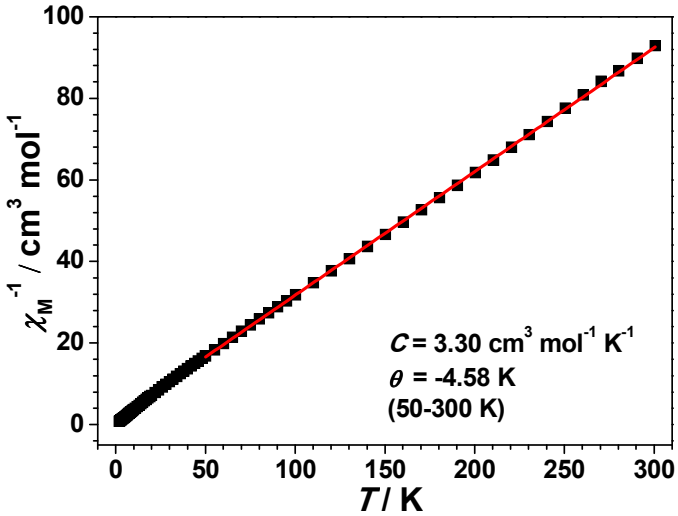

Figure S3. Plots of χ_M^{-1} *vs*. *T* for **2*R*** under 1 kOe dc field (The red solid line represents the best fit to the Curie-Weiss expression).

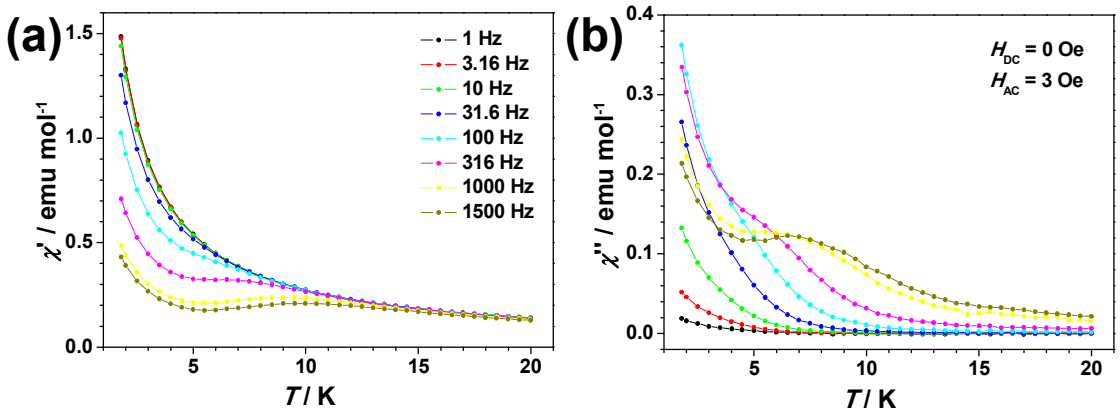

Figure S4. Temperature dependence of ac susceptibility (a) in-phase and (b) out-of-phase of **2*R*** in the absence of dc field at frequencies from 1 Hz to 1500 Hz in MPMS.

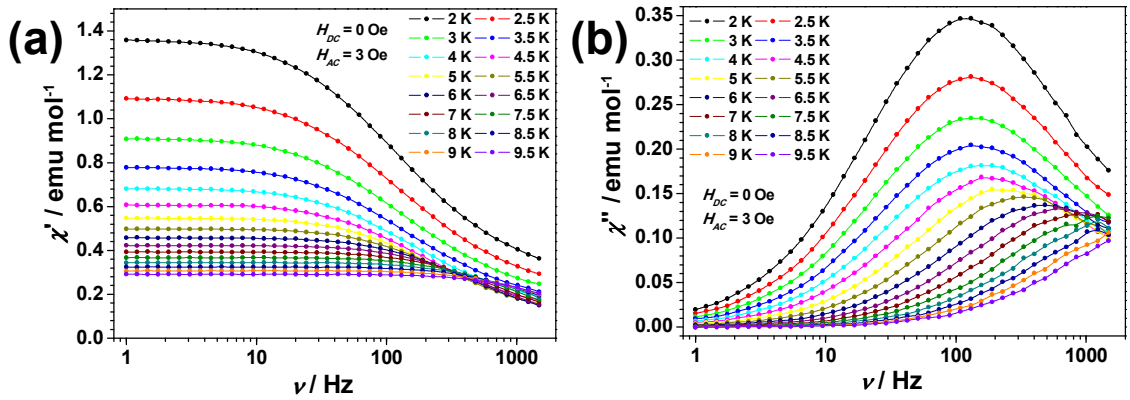

Figure S5. Frequency dependence (1-1500 Hz) of ac susceptibility (a) in-phase and (b) out-of-phase of **2*R*** in the absence of dc field at temperatures from 2 K to 9.5 K in MPMS.

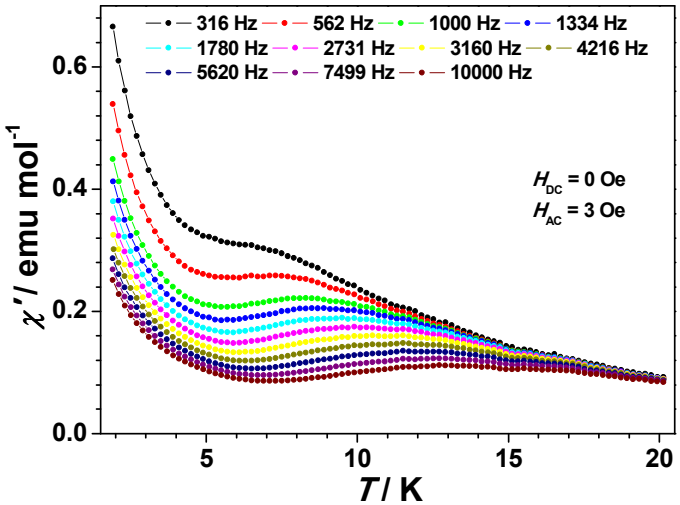

Figure S6. Temperature dependence of χ' (in-phase) of **2*R*** in the absence of dc field at temperatures from 1.9 K to 20.1 K in PPMS.

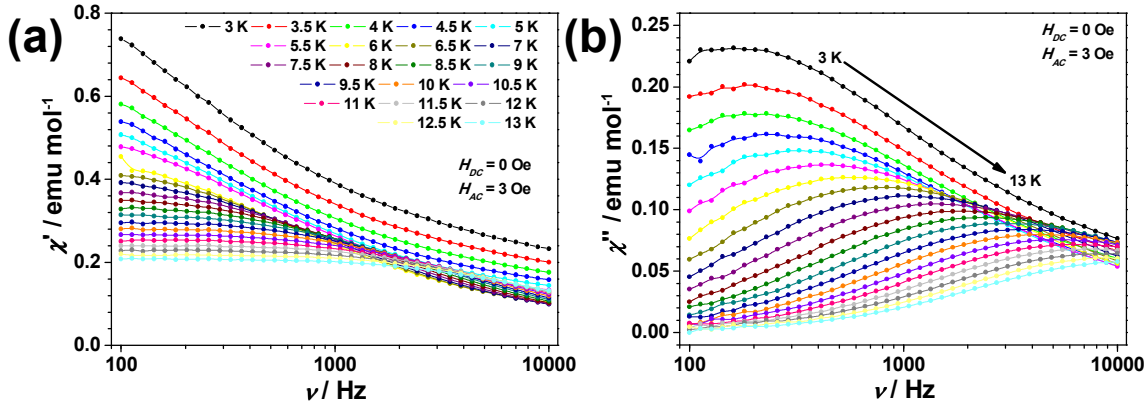

Figure S7. Frequency dependence (100-10000 Hz) of ac susceptibility (a) in-phase and (b) out-of-phase of **2*R*** in the absence of dc field at different temperatures (2 K to 9.5 K, 0.5 K interval) in PPMS.

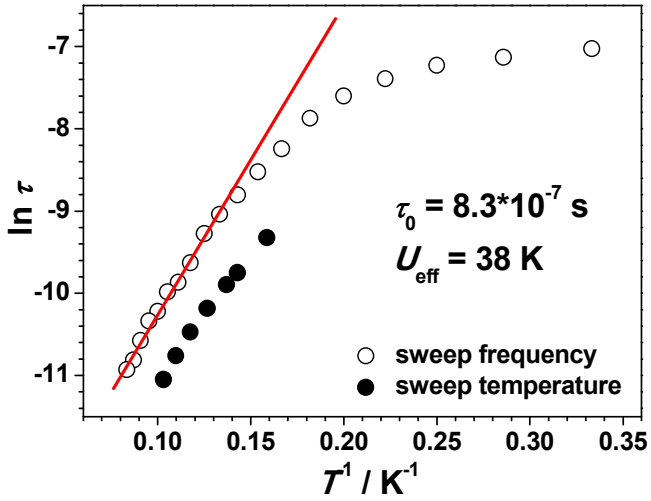

Figure S8. Arrhenius plots of relaxation times of **2*R*** in the absence of dc field, the data was collected from the peaks of χ'' (out-of-phase) against temperature and the peaks of χ'' (out-of-phase) against frequency at different temperatures.

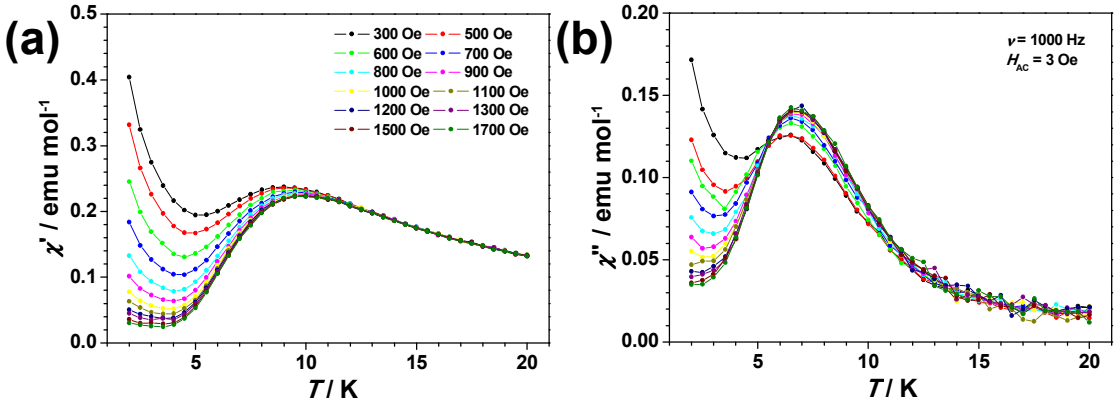

Figure S9. The temperature dependence of ac susceptibility of **2*R*** under different dc fields at frequency of 1000 Hz in MPMS, which reveals 1500 Oe dc field is the optimal applied field for suppression of QTM.

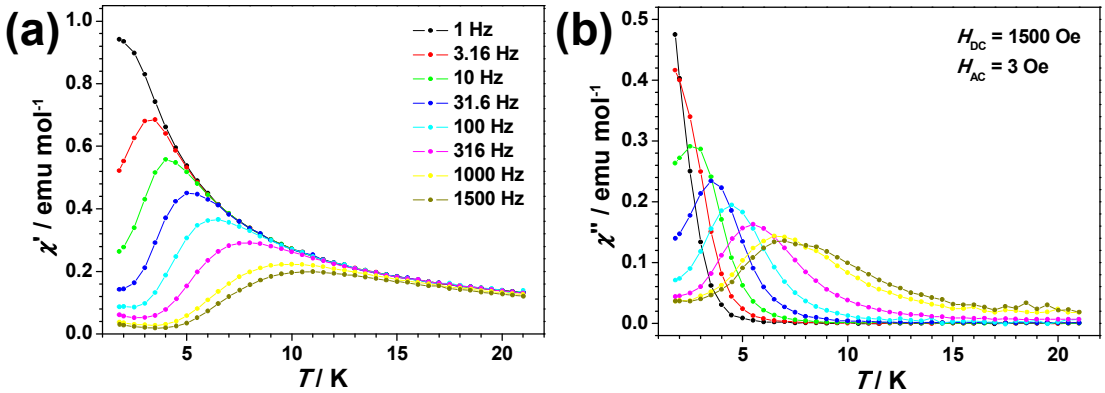

Figure S10. Temperature dependence of ac susceptibility of **2*R*** under a dc field of 1500 Oe at frequencies from 1 Hz to 1500 Hz in MPMS.

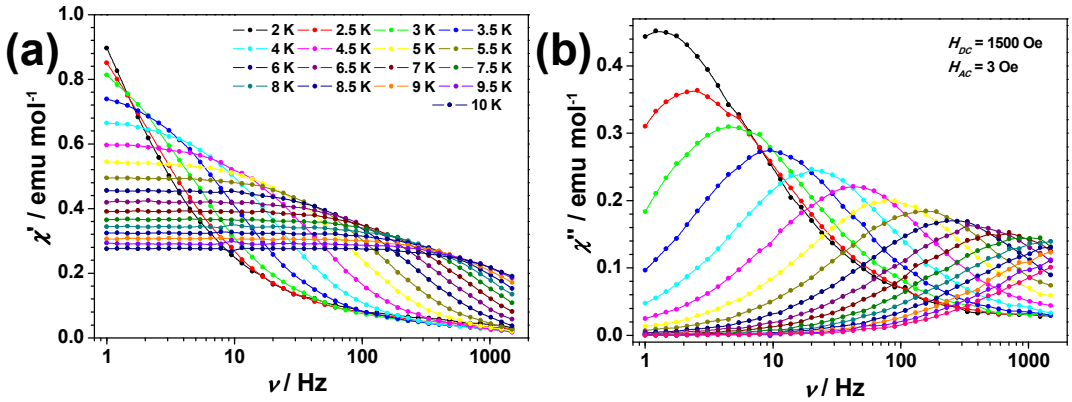

Figure S11. Frequency dependence (1-1500 Hz) of ac susceptibility (a) in-phase and (b) out-of-phase of **2*R*** under a dc field of 1500 Oe in MPMS.

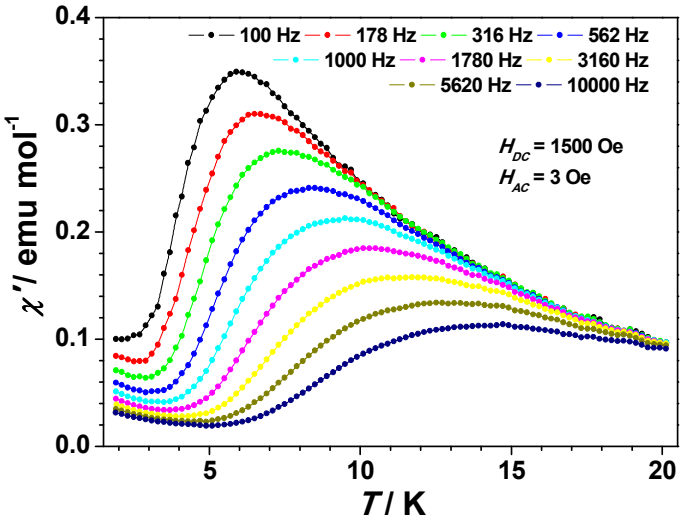

Figure S12. Temperature dependence of χ' (in-phase) of **2*R*** under a dc field of 1500 Oe range from 1.9 K to 20.1 K in PPMS.

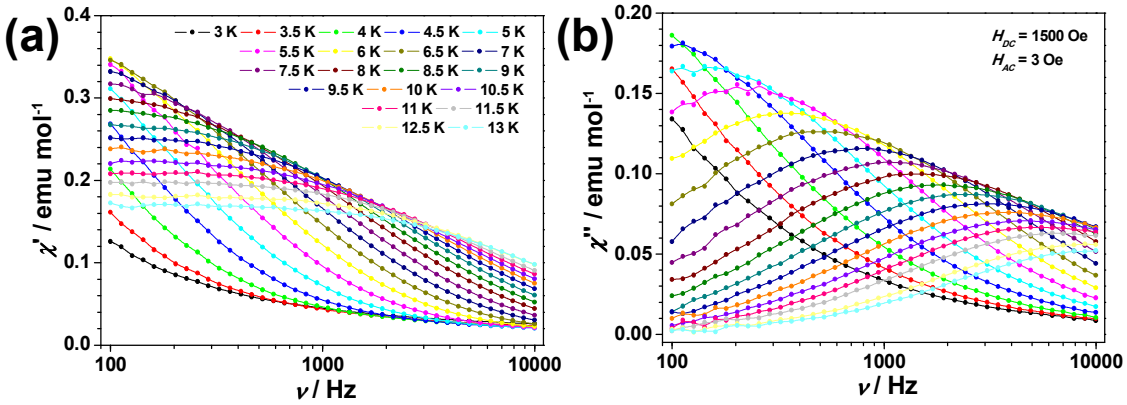

Figure S13. Frequency dependence (100-10000 Hz) of ac susceptibility (a) in-phase and (b) out-of-phase of **2*R*** under a dc field of 1500 Oe at different temperatures (2 K to 9.5 K, 0.5 K interval) in PPMS.

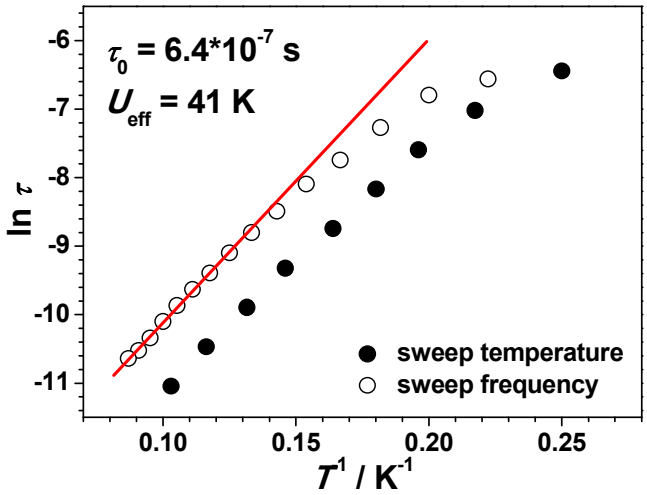

Figure S14. Arrhenius plots of relaxation times of **2*R*** under a dc field of 1500 Oe, the data was collected from the peaks of χ'' (out-of-phase) against temperature and the peaks of χ'' (out-of-phase) against frequency at different temperatures.

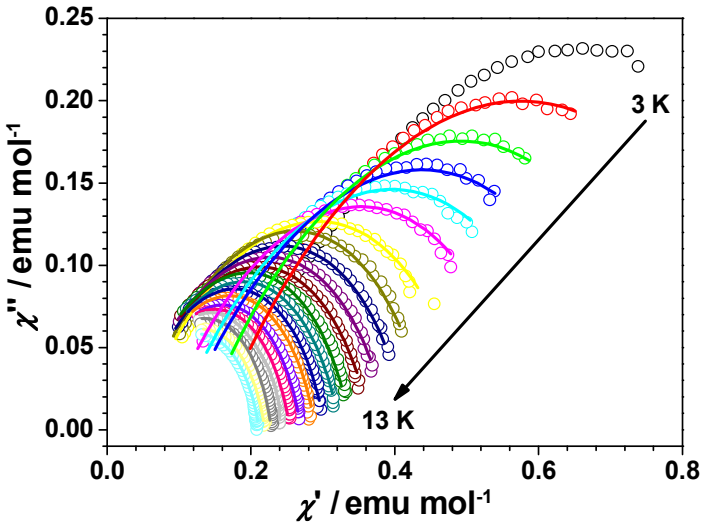

Figure S15. Cole-Cole diagram of **2*R*** in the absence of dc field (ac frequencies from 100 Hz to 10000 Hz, 0.5 K interval).

Table S9. The parameters of Cole-Cole fitting of **2*R*** in the absence of dc field.

T (K)	X_0	X_t	τ (s)	α	R
3.5	0.14925	0.93289	0.00094	0.39969	5.05×10^{-4}
4.0	0.12822	0.79635	0.00074	0.38421	4.47×10^{-4}
4.5	0.09878	0.72217	0.00063	0.40279	3.23×10^{-4}
5.0	0.09080	0.65239	0.00053	0.38891	2.44×10^{-4}
5.5	0.07683	0.58503	0.00039	0.37579	2.06×10^{-4}
6.0	0.03831	0.50784	0.00026	0.37036	4.36×10^{-4}
6.5	0.04012	0.44805	0.00018	0.31946	3.81×10^{-4}
7.0	0.03401	0.41963	0.00014	0.33165	2.86×10^{-4}
7.5	0.02614	0.39284	0.00010	0.33859	3.65×10^{-4}
8.0	0.02619	0.36719	0.00008	0.33019	3.73×10^{-4}
8.5	0.02704	0.33882	0.00006	0.30078	4.18×10^{-4}
9.0	0.02909	0.32391	0.00005	0.30278	2.72×10^{-4}
9.5	0.02935	0.30266	0.00004	0.28766	3.15×10^{-4}
10.0	0.03159	0.28951	0.00004	0.28249	3.07×10^{-4}
10.5	0.03297	0.26954	0.00003	0.27368	2.94×10^{-4}
11	0.02869	0.25425	0.00002	0.26615	3.95×10^{-4}
11.5	0.03140	0.23932	0.00002	0.23392	4.20×10^{-4}
12	0.03041	0.22835	0.00002	0.23659	3.57×10^{-4}
12.5	0.03023	0.21949	0.00002	0.26996	3.32×10^{-4}
13	0.03194	0.21128	0.00002	0.26867	3.60×10^{-4}

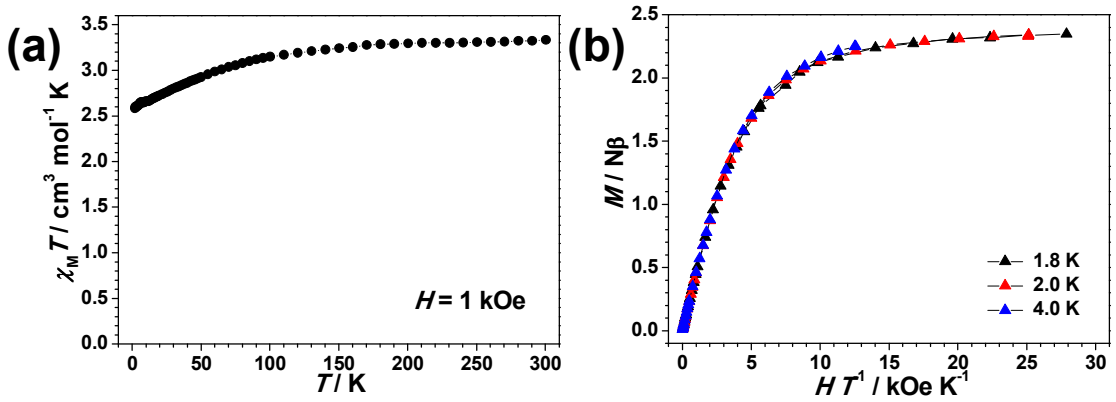

Figure S16. (a) Temperature dependence of $\chi_M T$ of **2*S*** at H = 1 kOe from 2–300 K; (b), M *vs.* H/T plots at different temperatures (1.8 K, 2 K, and 4 K) of **2*S*** in MPMS.

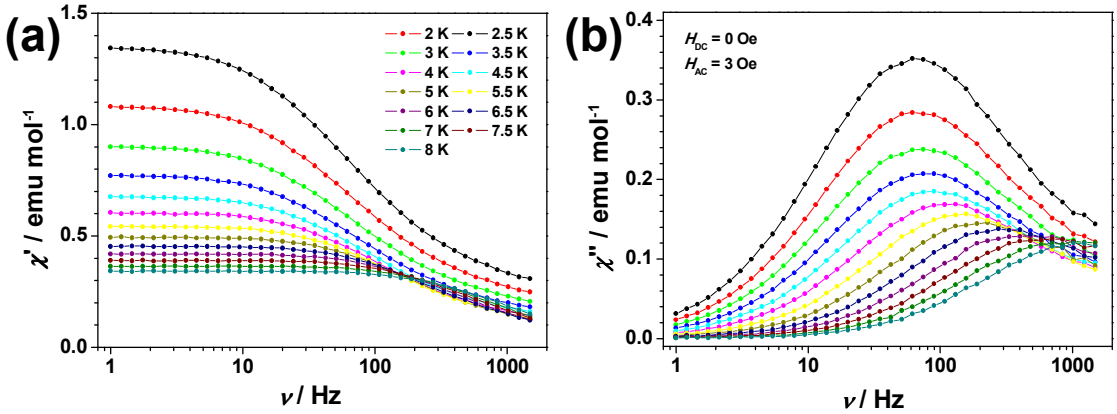

Figure S17. Frequency dependence (1-1500 Hz) of ac susceptibility (a) in-phase and (b) out-of-phase of **2*S*** in the absence of dc field at temperatures from 2 K to 8 K in MPMS.

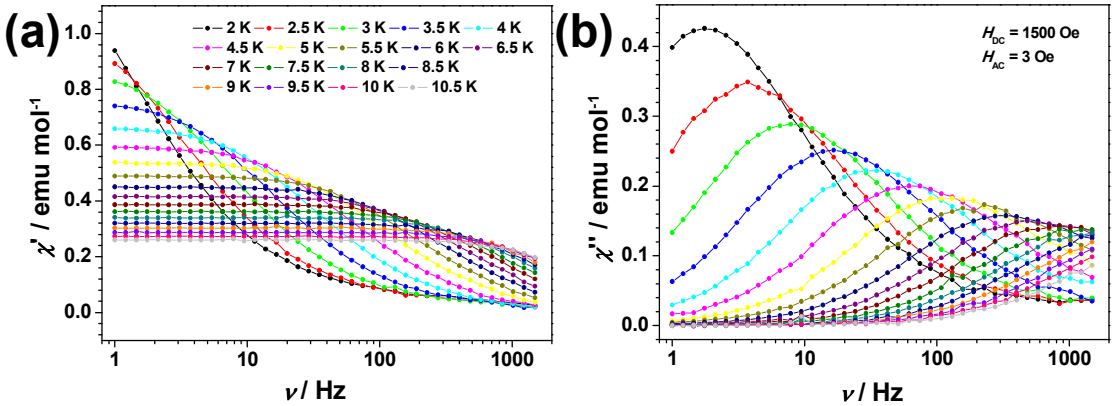

Figure S18. Frequency dependence (1-1500 Hz) of ac susceptibility (a) in-phase and (b) out-of-phase of **2*S*** under a dc field of 1500 Oe at temperatures from 2 K to 10.5 K in MPMS.

The magnetic data of compound 3*R*.

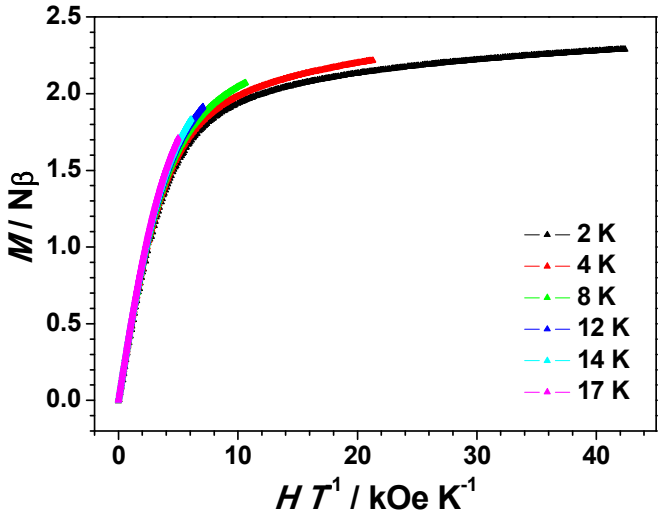

Figure S19. *M vs. H*/*T* plots of **3*R*** at different temperatures (2 K, 4 K, 8 K, 12 K, 14 K, and 17 K). It is found that the bifurcation of curves is significant at high field range.

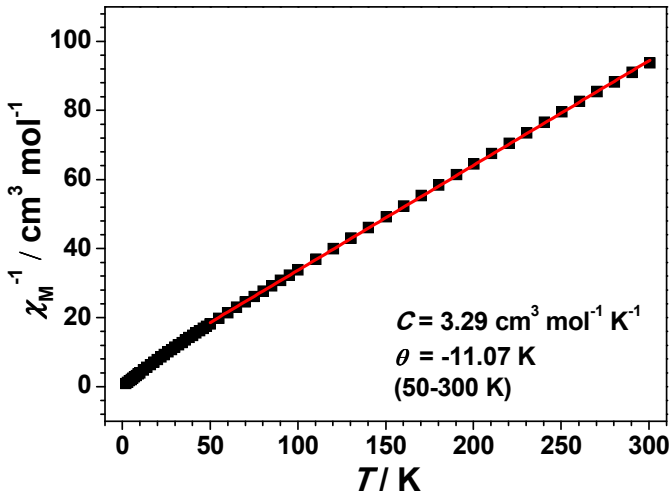

Figure S20. Plots of χ_M^{-1} *vs. T* for **3*R*** under 1 kOe dc field (The red solid line represents the best fit to the Curie-Weiss expression).

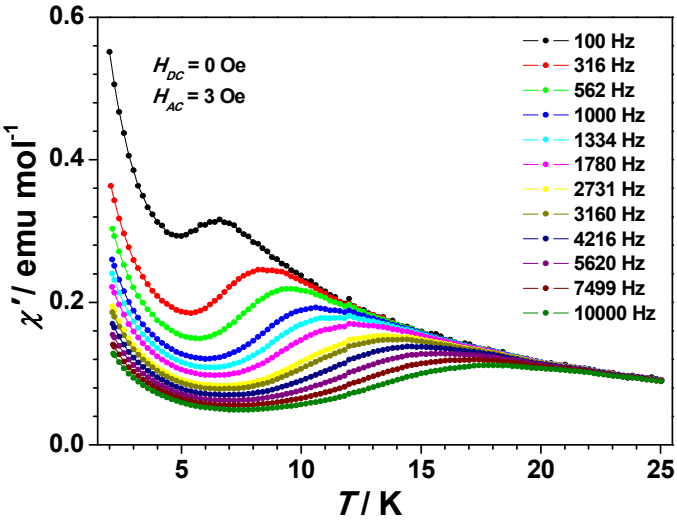

Figure S21. Temperature dependence of χ' (in-phase) of **3*R*** in the absence of dc field at temperatures from 2 K to 25 K in PPMS.

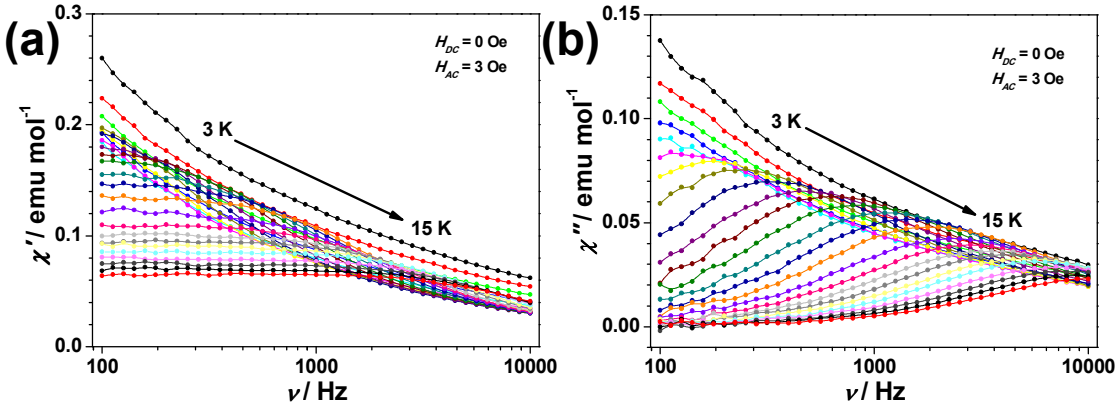

Figure S22. Frequency dependence (100-10000 Hz) of ac susceptibility (a) in-phase and (b) out-of-phase of **3*R*** in the absence of dc field at different temperatures (3 K to 15 K, 0.5 K interval) in PPMS.

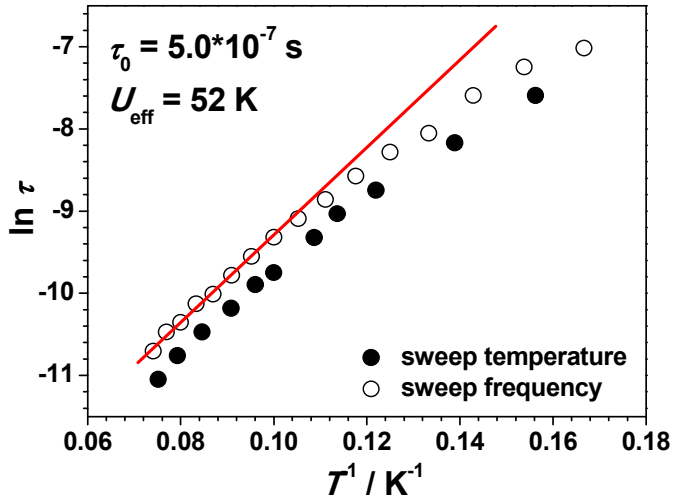

Figure S23. Arrhenius plots of relaxation times of **3*R*** in the absence of dc field, the data was collected from the peaks of χ'' (out-of-phase) against temperature and the peaks of χ'' (out-of-phase) against frequency at different temperatures.

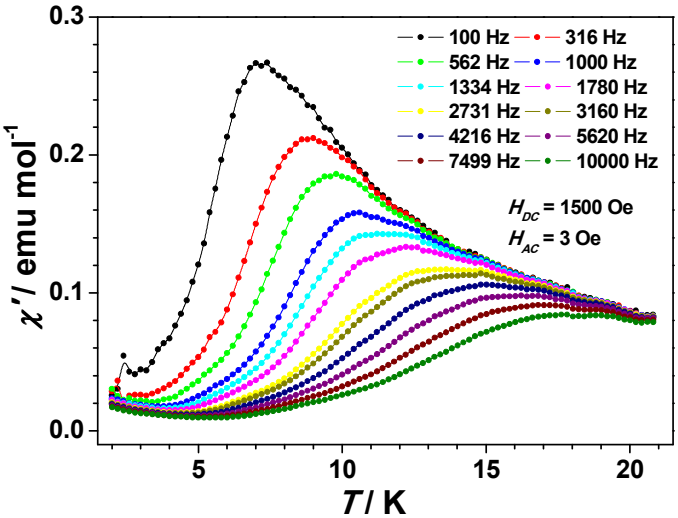

Figure S24. Temperature dependence of χ' (in-phase) of **3*R*** under a dc field of 1500 Oe range from 2.0 K to 20.8 K in PPMS.

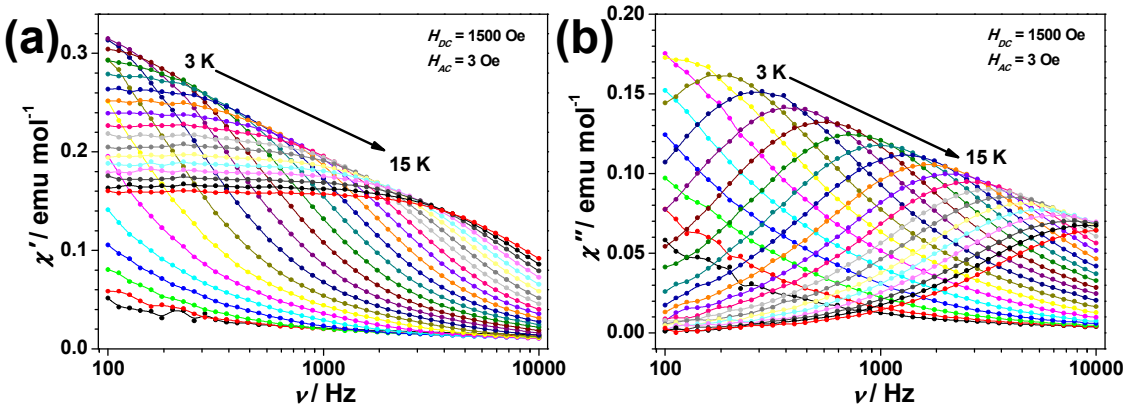

Figure S25. Frequency dependence (100-10000 Hz) of ac susceptibility (a) in-phase and (b) out-of-phase of **3*R*** under a dc field of 1500 Oe at different temperatures (3 K to 15 K, 0.5 K interval) in PPMS.

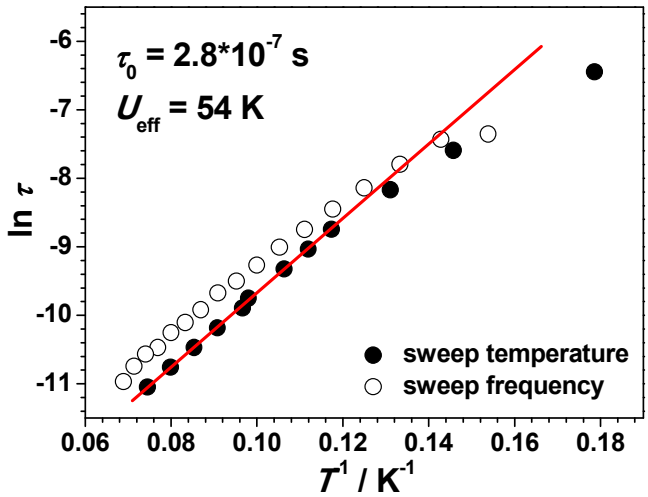

Figure S26. Arrhenius plots of relaxation times of **3*R*** under a dc field of 1500 Oe, the data was collected from the peaks of χ'' (out-of-phase) against temperature and the peaks of χ'' (out-of-phase) against frequency at different temperatures.

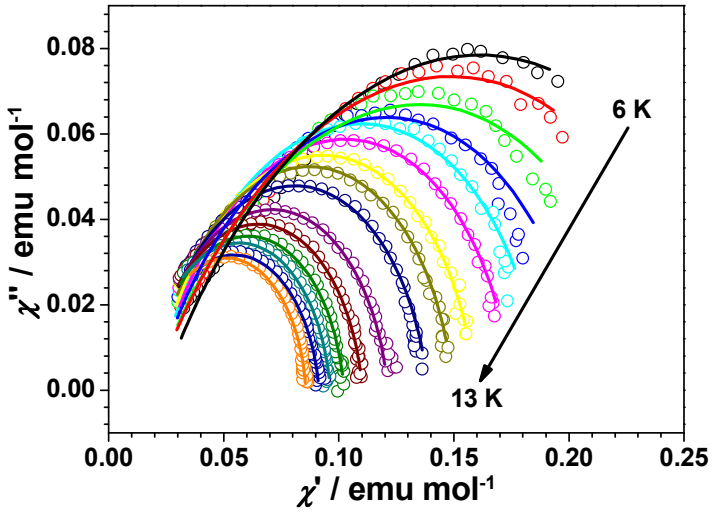

Figure S27. Cole-Cole diagram of **3*R*** in the absence of dc field from 6 K to 13 K (ac frequencies from 100 Hz to 10000 Hz, 0.5 K interval).

Table S10. The parameters of Cole-Cole fitting of **3*R*** in the absence of dc field.

T (K)	X_0	X_t	τ (s)	α	R
6.0	0.02296	0.27820	0.00096	0.29791	2.96×10^{-3}
6.5	0.01947	0.25848	0.00069	0.29829	1.83×10^{-3}
7.0	0.01922	0.23322	0.00050	0.28849	1.43×10^{-3}
7.5	0.01926	0.20819	0.00031	0.24288	1.49×10^{-3}
8.0	0.02025	0.18901	0.00023	0.18909	1.06×10^{-3}
8.5	0.02114	0.17587	0.00017	0.17294	8.99×10^{-4}
9.0	0.02022	0.15957	0.00013	0.14878	8.03×10^{-4}
9.5	0.01921	0.14975	0.00010	0.13903	4.75×10^{-4}
10.0	0.01709	0.13872	0.00009	0.15085	6.12×10^{-4}
10.5	0.01634	0.12131	0.00006	0.13619	6.94×10^{-4}
11.0	0.01634	0.11024	0.00006	0.11907	5.83×10^{-4}
11.5	0.01649	0.10221	0.00005	0.10894	6.56×10^{-4}
12.0	0.01517	0.09622	0.00004	0.10228	5.50×10^{-4}
12.5	0.01493	0.09142	0.00003	0.11901	3.90×10^{-4}
13.0	0.01575	0.08564	0.00003	0.07649	6.49×10^{-4}

The magnetic data of compound 4*R*.

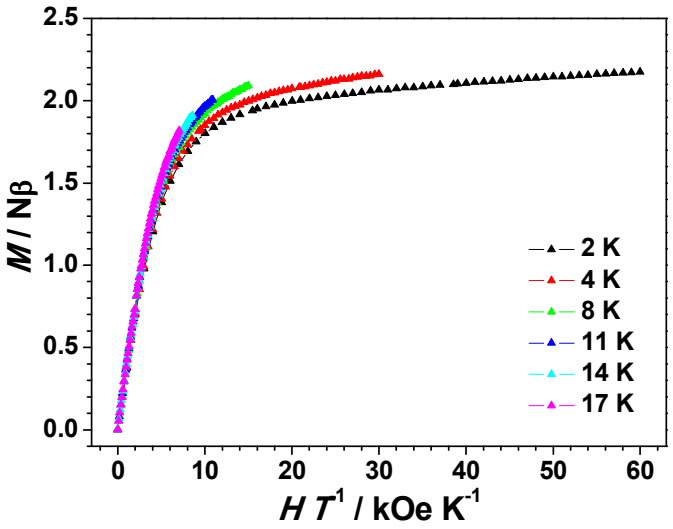

Figure S28. *M vs*. *H*/*T* plots of **4*R*** at different temperatures (2 K, 4 K, 8 K, 12 K, 14 K, and 17 K). It is found that the bifurcation of curves is significant at high field range.

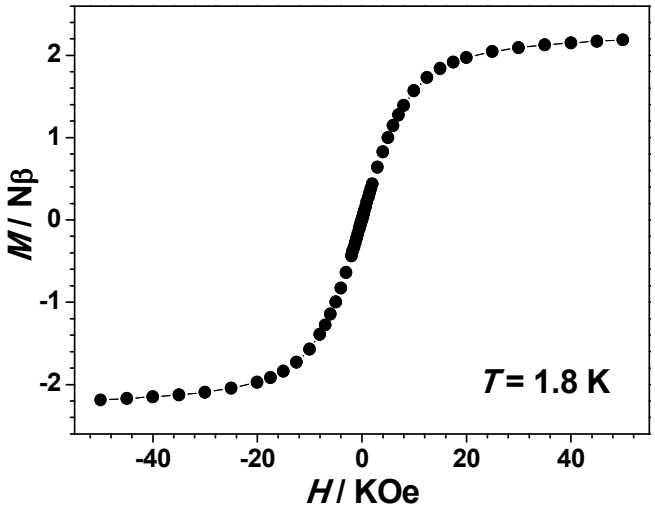

Figure S29. Magnetization *vs*. field measured for the **4*R*** at 1.8 K from -50 kOe to 50 kOe in MPMS, no hysteresis loop was observed.

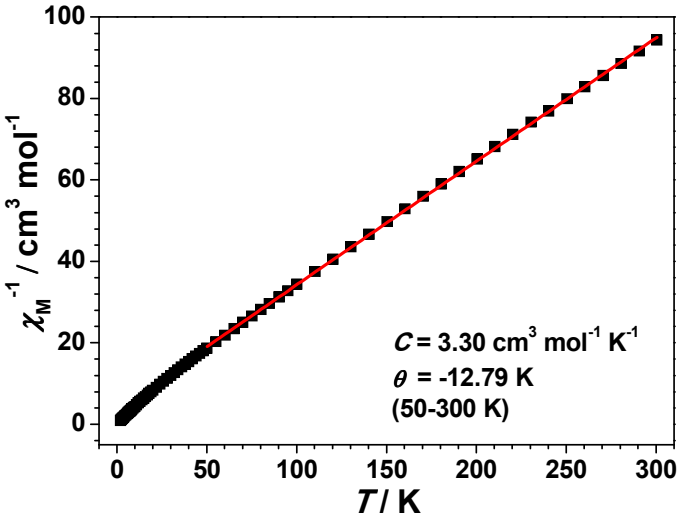

Figure S30. Plots of χ_M^{-1} *vs*. *T* for **4*R*** under 1 kOe dc field (The red solid line represents the best fit to the Curie-Weiss expression).

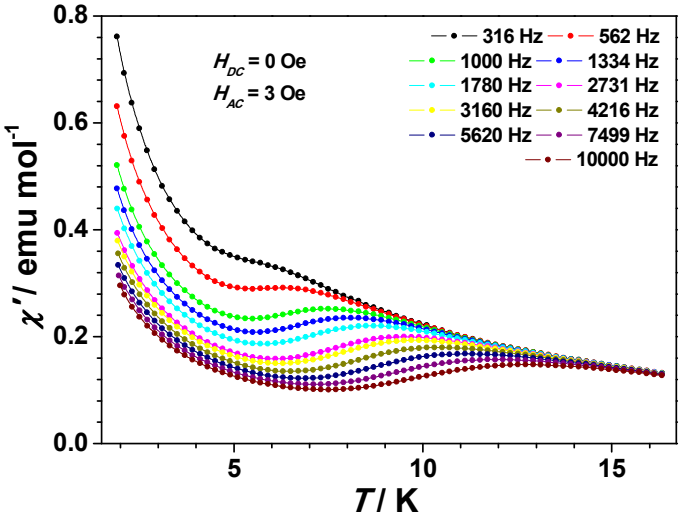

Figure S31. Temperature dependence of χ' (in-phase) of **4*R*** in the absence of dc field range from 1.9 K to 16.3 K in PPMS.

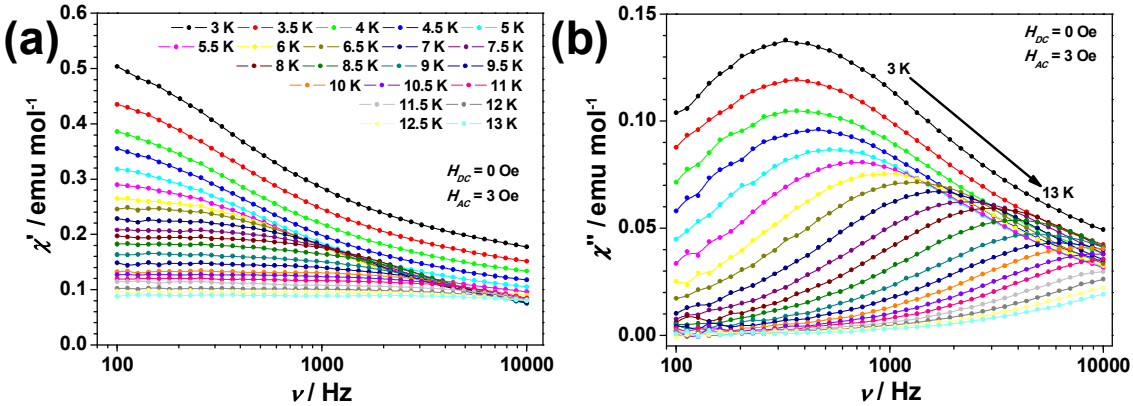

Figure S32. Frequency dependence (100-10000 Hz) of ac susceptibility (a) in-phase and (b) out-of-phase of **4*R*** in the absence of dc field at different temperatures (2 K to 9.5 K, 0.5 K interval) in PPMS.

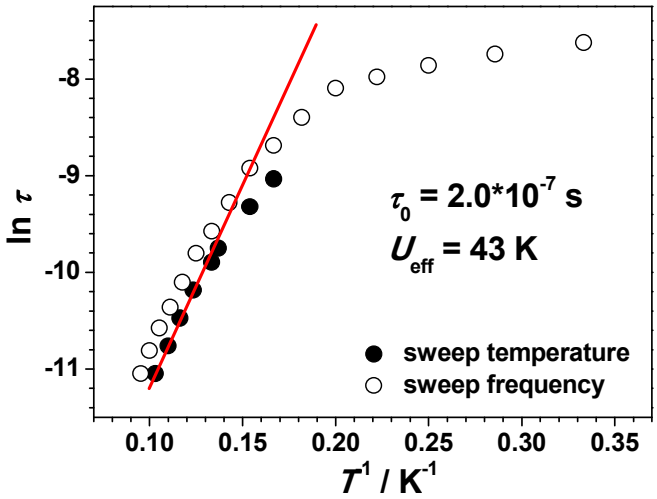

Figure S33. Arrhenius plots of relaxation times of **4*R*** in the absence of dc field, the data was collected from the peaks of χ'' (out-of-phase) against temperature and the peaks of χ'' (out-of-phase) against frequency at different temperatures.

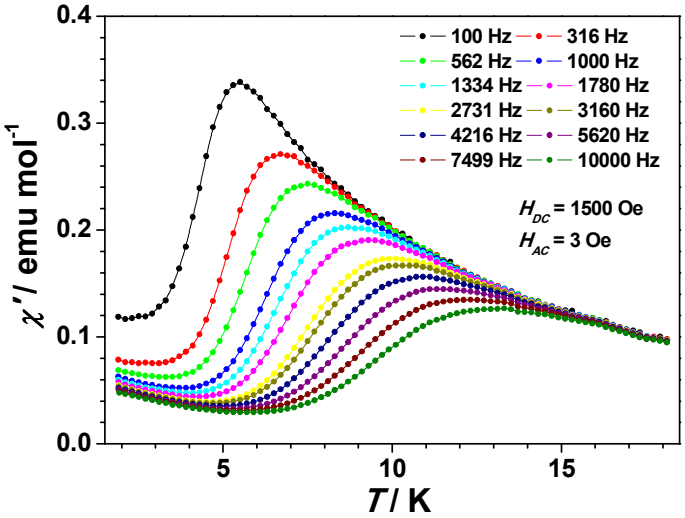

Figure S34. Temperature dependence of χ' (in-phase) of **4*R*** under a dc field of 1500 Oe range from 1.9 K to 18.1 K in PPMS.

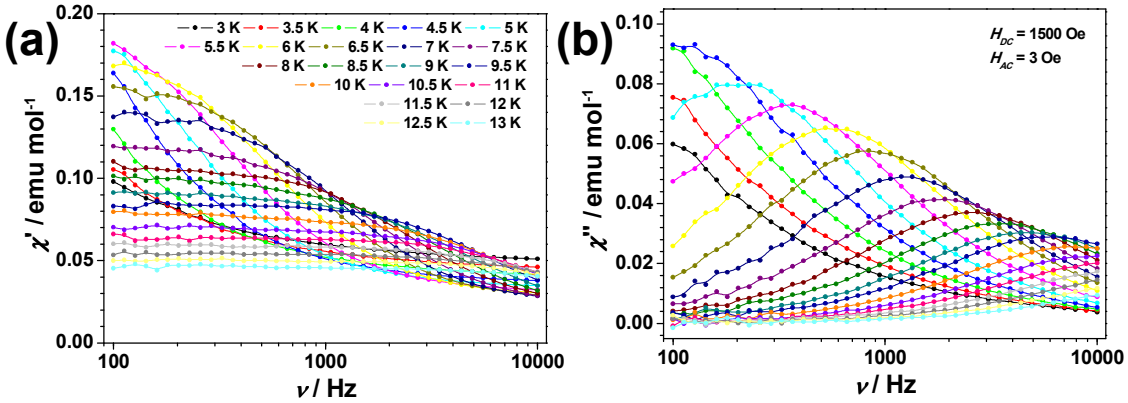

Figure S35. Frequency dependence (100-10000 Hz) of ac susceptibility (a) in-phase and (b) out-of-phase of **4*R*** under a dc field of 1500 Oe at different temperatures (3 K to 13 K, 0.5 K interval) in PPMS.

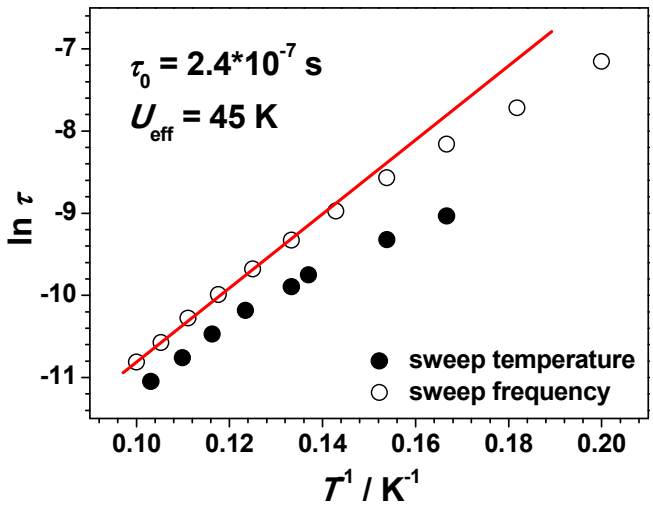

Figure S36. Arrhenius plots of relaxation times of **4*R*** under a dc field of 1500 Oe, the data was collected from the peaks of χ'' (out-of-phase) against temperature and the peaks of χ'' (out-of-phase) against frequency at different temperatures.

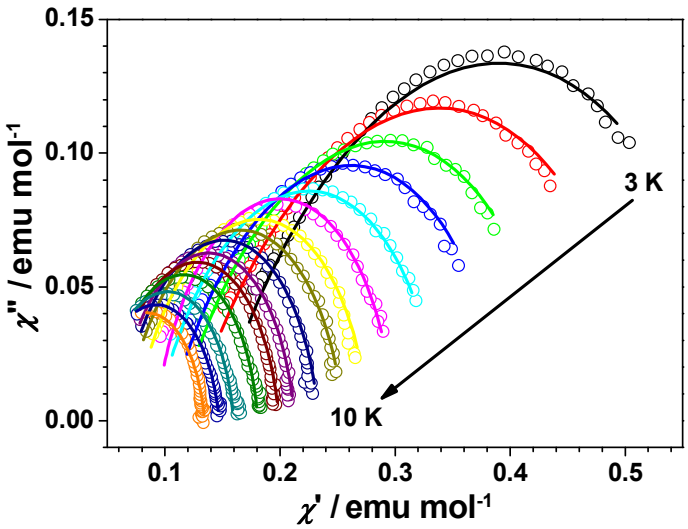

Figure S37. Cole-Cole diagram of **4*R*** in the absence of dc field from 3 K to 10 K (ac frequencies from 100 to 10000 Hz, 0.5 K interval).

Table S11. The parameters of Cole-Cole fitting of **4*R*** in the absence of dc field.

T (K)	X_0	X_t	τ (s)	α	R
3.0	0.14290	0.59824	0.00046	0.32409	3.81×10^{-4}
3.5	0.12083	0.52138	0.00044	0.32758	2.68×10^{-4}
4.0	0.10910	0.44565	0.00040	0.29301	4.15×10^{-4}
4.5	0.10212	0.39803	0.00037	0.27064	4.27×10^{-4}
5.0	0.09144	0.34133	0.00027	0.23385	3.83×10^{-4}
5.5	0.09086	0.30023	0.00022	0.14669	5.91×10^{-4}
6.0	0.07244	0.27803	0.00016	0.19554	3.63×10^{-4}
6.5	0.06401	0.25571	0.00012	0.18579	3.10×10^{-4}
7.0	0.06093	0.23363	0.00009	0.15537	3.13×10^{-4}
7.5	0.05787	0.21252	0.00007	0.13265	2.54×10^{-4}
8.0	0.05075	0.19905	0.00005	0.14186	2.51×10^{-4}
8.5	0.04734	0.18069	0.00004	0.12636	2.79×10^{-4}
9.0	0.04000	0.15964	0.00003	0.13574	6.37×10^{-4}
9.5	0.03086	0.14728	0.00003	0.18535	6.76×10^{-4}
10.0	0.02906	0.13454	0.00002	0.16907	3.16×10^{-4}

The magnetic data of compound 5*R*.

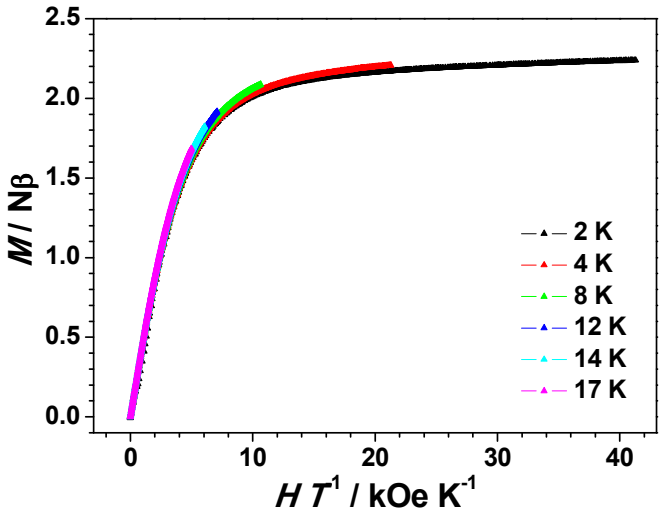

Figure S38. *M vs. H*/*T* plots of **5*R*** at different temperatures (2 K, 4 K, 8 K, 12 K, 14 K, and 17 K). It is found that the bifurcation of curves is significant at high field range.

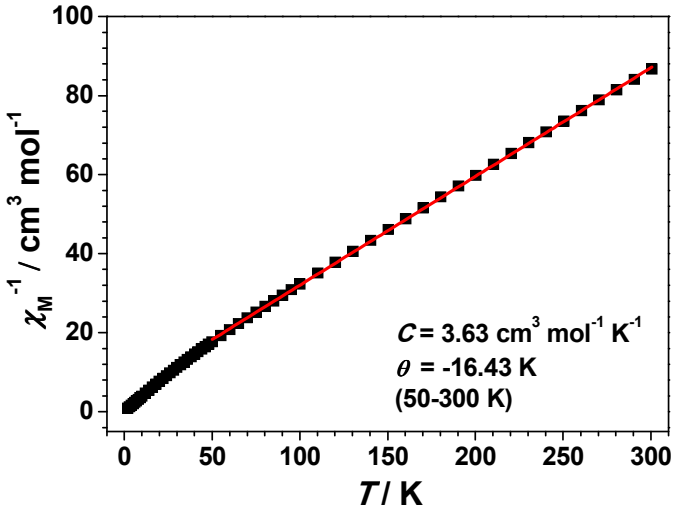

Figure S39. Plots of χ_M^{-1} *vs. T* for **5*R*** under 1 kOe dc field (The red solid line represents the best fit to the Curie-Weiss expression).

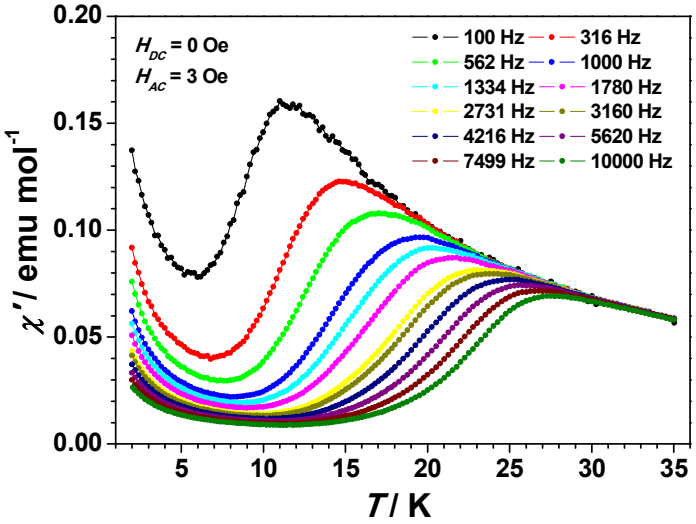

Figure S40. Temperature dependence of χ' (in-phase) of **5*R*** in the absence of dc field range from 2.0 K to 35.0 K in PPMS.

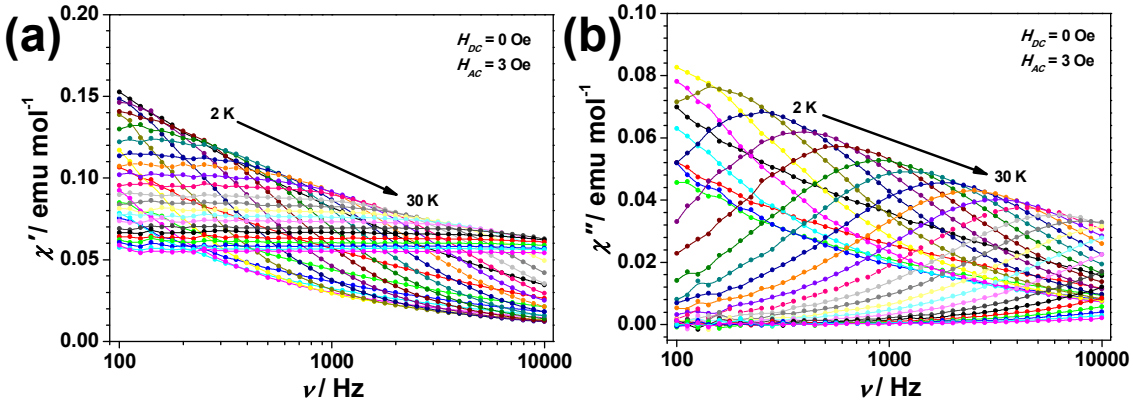

Figure S41. Frequency dependence (100-10000 Hz) of ac susceptibility (a) in-phase and (b) out-of-phase of **5*R*** in the absence of dc field at different temperatures (2 K to 30 K, 1 K interval) in PPMS.

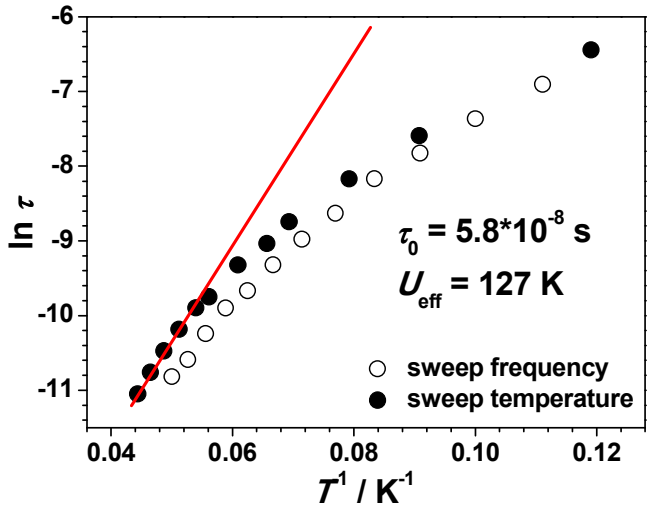

Figure S42. Arrhenius plots of relaxation times of **5*R*** in the absence of dc field, the data was collected from the peaks of χ'' (out-of-phase) against temperature and the peaks of χ'' (out-of-phase) against frequency at different temperatures.

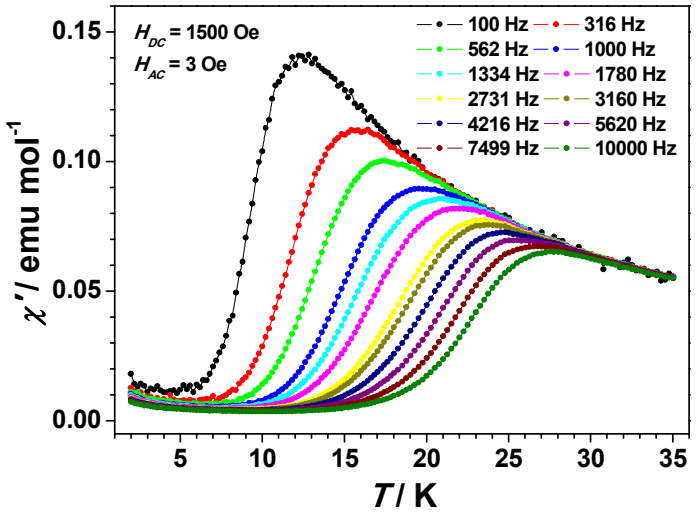

Figure S43. Temperature dependence of χ' (in-phase) of **5*R*** under a dc field of 1500 Oe range from 2.0 K to 35.0 K in PPMS.

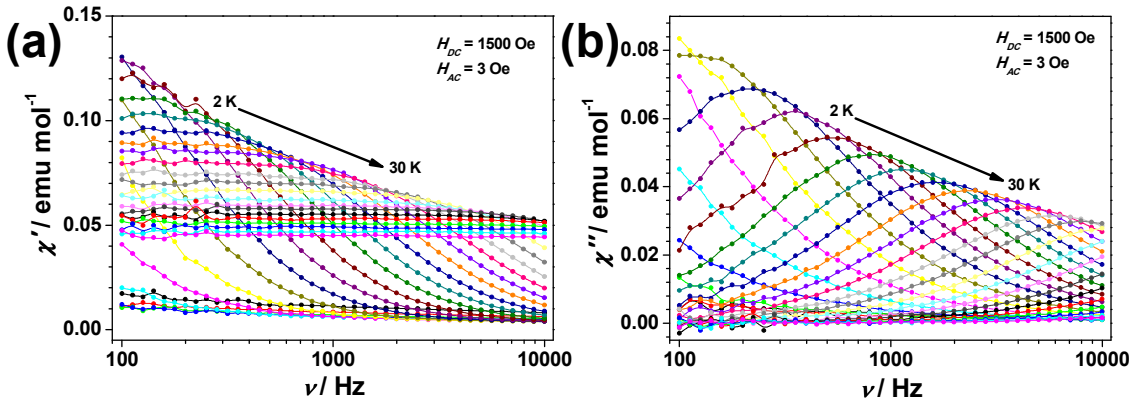

Figure S44. Frequency dependence (100-10000 Hz) of ac susceptibility (a) in-phase and (b) out-of-phase of **5*R*** under a dc field of 1500 Oe at different temperatures (2 K to 30 K, 1 K interval) in PPMS.

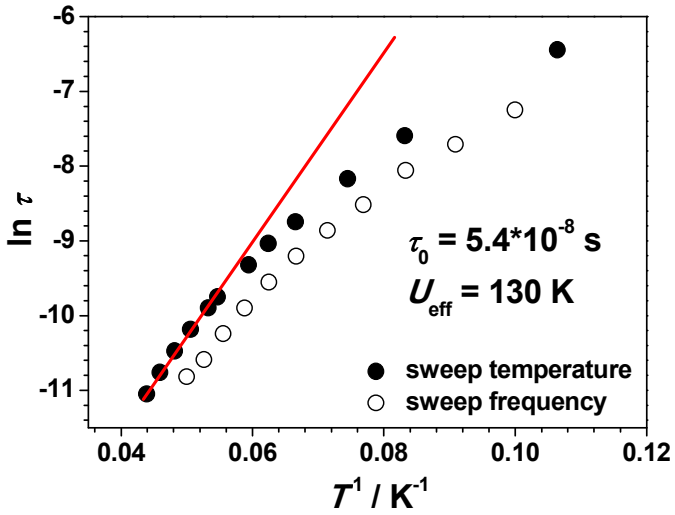

Figure S45. Arrhenius plots of relaxation times of **5*R*** under a dc field of 1500 Oe, the data was collected from the peaks of χ'' (out-of-phase) against temperature and the peaks of χ'' (out-of-phase) against frequency at different temperatures.

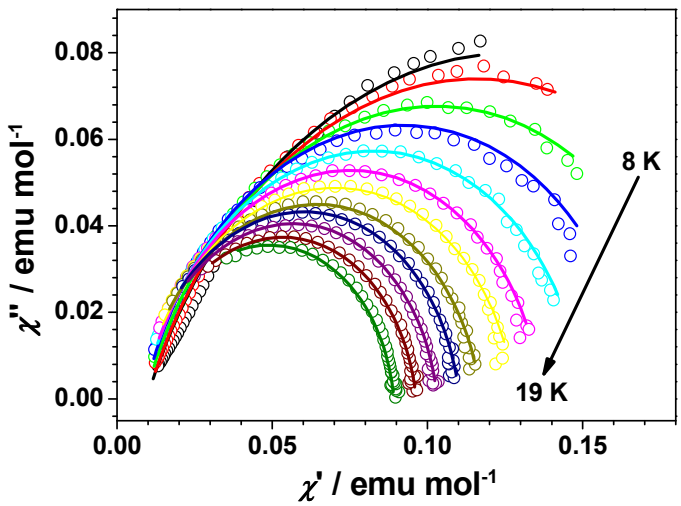

Figure S46. Cole-Cole diagram of **5*R*** in the absence of dc field from 8 K to 19 K (ac frequencies from 100 to 10000 Hz, 1 K interval).

Table S12. The parameters of Cole-Cole fitting of **5*R*** in the absence of dc field.

T (K)	X_0	X_t	τ (s)	α	R
8.0	0.00963	0.23032	0.00186	0.20213	3.77×10^{-3}
9.0	0.00970	0.21035	0.00105	0.19098	8.22×10^{-4}
10.0	0.00891	0.18725	0.00068	0.17353	6.64×10^{-4}
11.0	0.00853	0.16854	0.00042	0.14822	8.37×10^{-4}
12.0	0.00830	0.15076	0.00024	0.13777	1.30×10^{-3}
13.0	0.00853	0.13713	0.00018	0.12446	7.46×10^{-4}
14.0	0.00729	0.12846	0.00013	0.13647	1.37×10^{-3}
15.0	0.00703	0.11725	0.00009	0.12849	5.47×10^{-4}
16.0	0.00734	0.11033	0.00006	0.10999	2.64×10^{-4}
17.0	0.00755	0.10314	0.00005	0.10468	4.58×10^{-4}
18.0	0.00762	0.09638	0.00003	0.10892	3.79×10^{-4}
19.0	0.00708	0.08914	0.00002	0.09111	1.21×10^{-3}

The magnetic data of compound 6*R*.

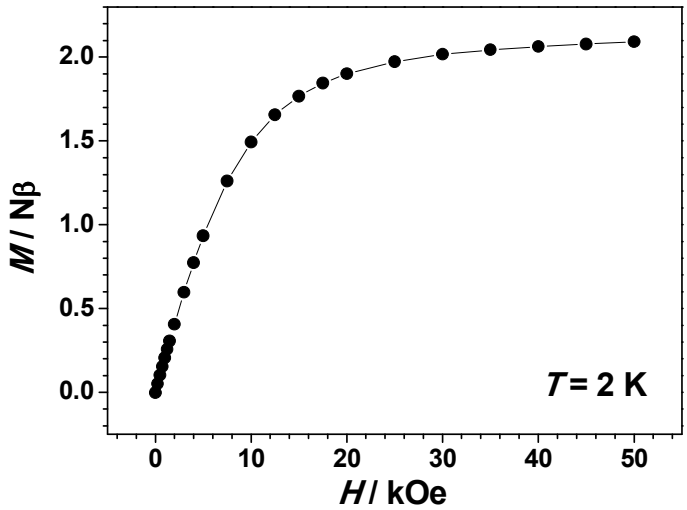

Figure S47. Isothermal magnetization for **6*R*** from 0 T to 5 T at 2.0 K.

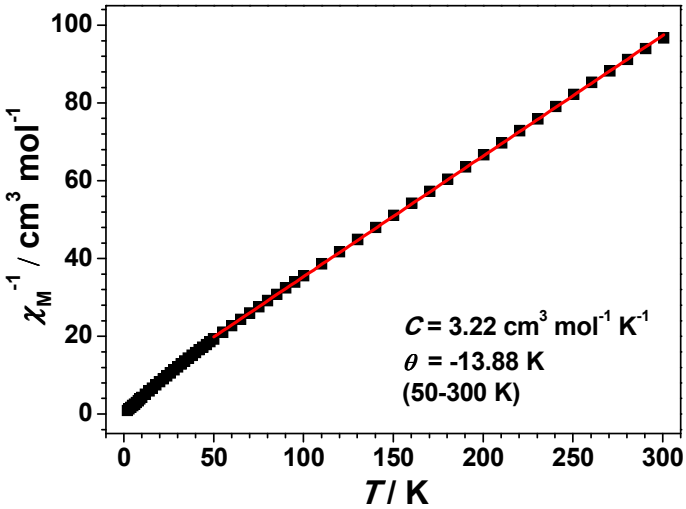

Figure S48. Plots of χ_M^{-1} *vs*. *T* for **6*R*** under 1 kOe dc field (The red solid line represents the best fit to the Curie-Weiss expression).

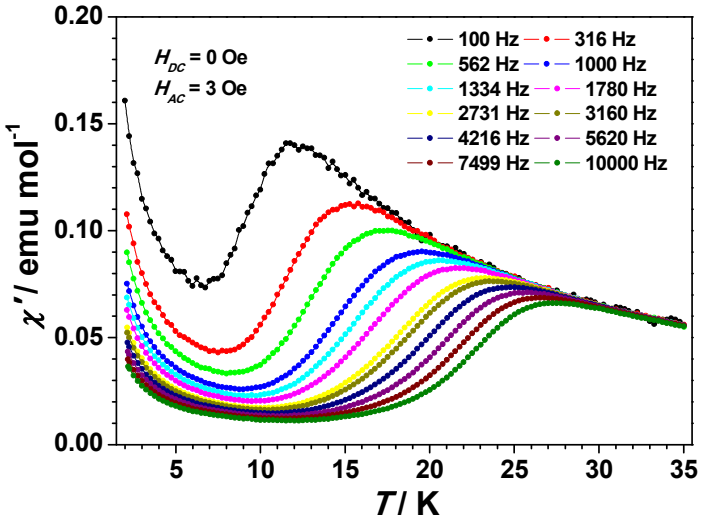

Figure S49. Temperature dependence of χ' (in-phase) of ***6R*** in the absence of dc field range from 2.0 K to 35.0 K in PPMS.

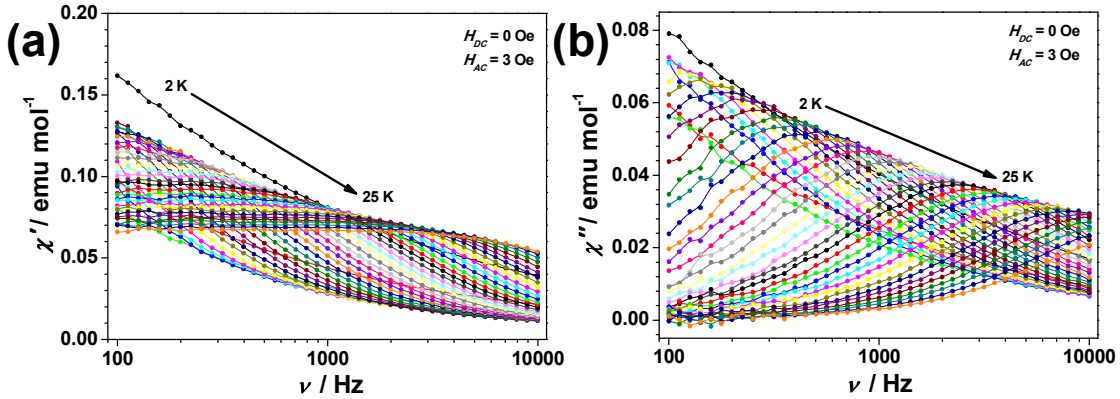

Figure S50. Frequency dependence (100-10000 Hz) of ac susceptibility (a) in-phase and (b) out-of-phase of ***6R*** in the absence of dc field at different temperatures (2 K to 8 K, 2 K interval, 8.5 K to 25 K, 0.5 K interval) in PPMS.

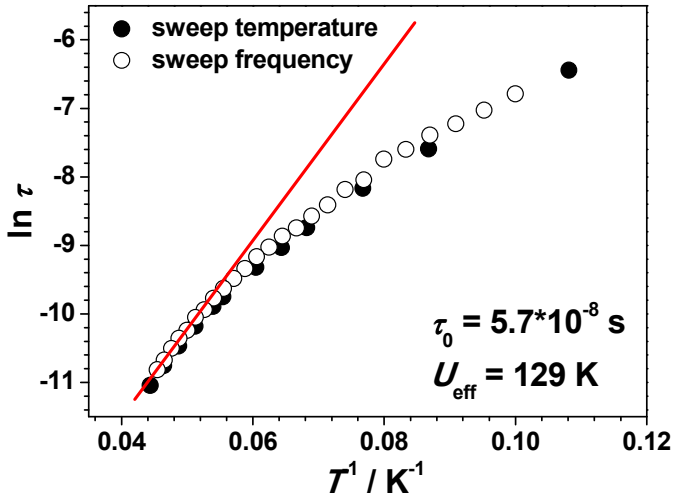

Figure S51. Arrhenius plots of relaxation times of **6*R*** in the absence of dc field, the data was collected from the peaks of χ'' (out-of-phase) against temperature and the peaks of χ'' (out-of-phase) against frequency at different temperatures.

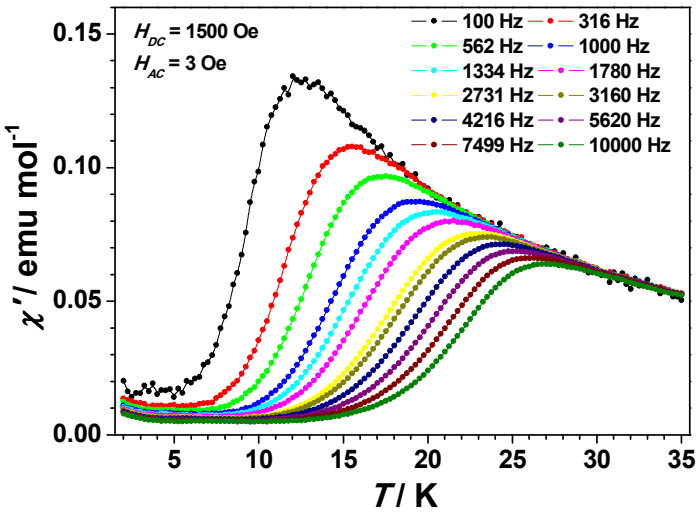

Figure S52. Temperature dependence of χ' (in-phase) of **6*R*** under a dc field of 1500 Oe range from 2.0 K to 35.0 K in PPMS.

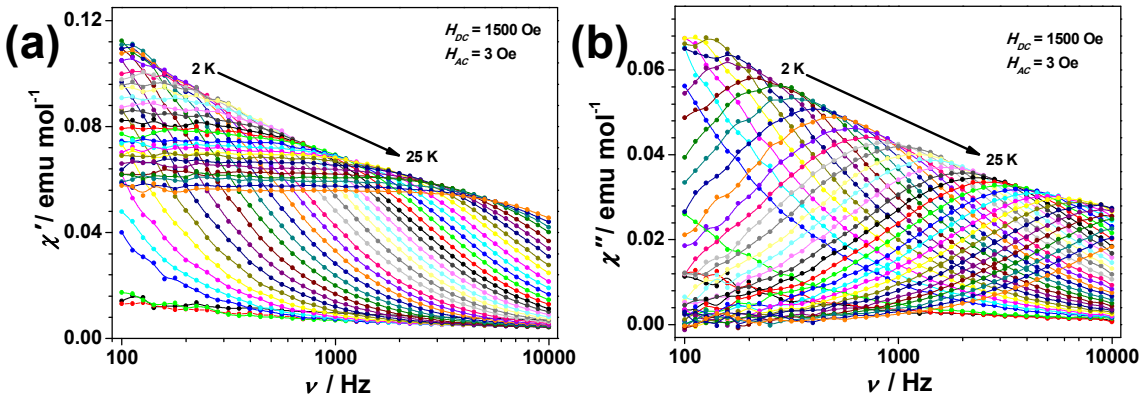

Figure S53. Frequency dependence (100-10000 Hz) of ac susceptibility (a) in-phase and (b) out-of-phase of ***6R*** under a dc field of 1500 Oe at different temperatures (2 K to 8 K, 2 K interval, 8.5 to 25 K, 0.5 K interval) in PPMS.

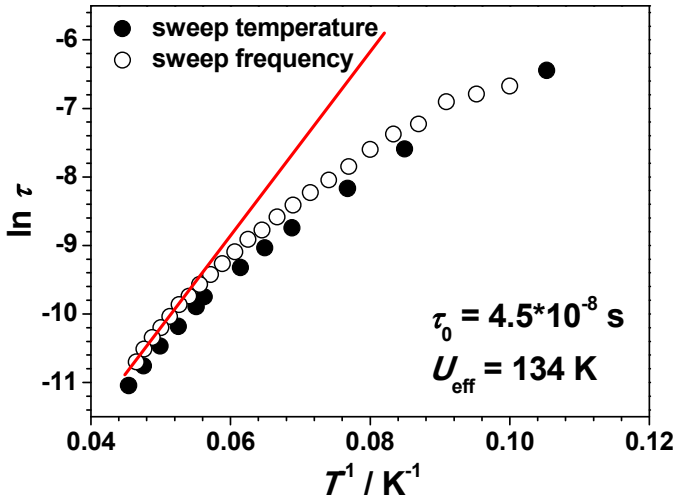

Figure S54. Arrhenius plots of relaxation times of ***6R*** under a dc field of 1500 Oe, the data was collected from the peaks of χ'' (out-of-phase) against temperature and the peaks of χ'' (out-of-phase) against frequency at different temperatures.

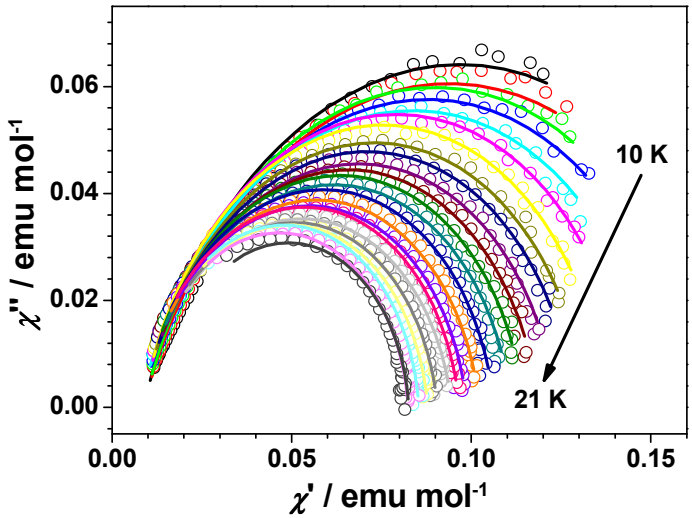

Figure S55. Cole-Cole diagram of **6*R*** in the absence of dc field from 10 K to 21 K (ac frequencies from 100 Hz to 10000 Hz, 0.5 K interval).

Table S13. The parameters of Cole-Cole fitting of **6*R*** in the absence of dc field.

T (K)	X_0	X_t	τ	α	R
10.0	0.00874	0.17633	0.00101	0.16856	2.38×10^{-3}
10.5	0.00872	0.17034	0.00087	0.18128	1.36×10^{-3}
11.0	0.00889	0.16321	0.00069	0.16004	9.55×10^{-4}
11.5	0.00776	0.15954	0.00055	0.17373	8.30×10^{-4}
12.0	0.00751	0.15257	0.00049	0.16846	8.82×10^{-4}
12.5	0.00824	0.14460	0.00036	0.13806	9.17×10^{-4}
13.0	0.00845	0.13781	0.00030	0.12859	6.00×10^{-4}
13.5	0.00819	0.13239	0.00025	0.14327	6.40×10^{-4}
14.0	0.00817	0.12889	0.00021	0.14689	8.37×10^{-4}
14.5	0.00812	0.12392	0.00018	0.15116	8.95×10^{-4}
15.0	0.00819	0.11885	0.00015	0.13876	6.90×10^{-4}
15.5	0.00811	0.11476	0.00014	0.13113	5.70×10^{-4}
16.0	0.00810	0.11125	0.00012	0.13542	7.58×10^{-4}
16.5	0.00810	0.10639	0.00009	0.11921	9.75×10^{-4}
17.0	0.00803	0.10235	0.00009	0.12375	5.92×10^{-4}
17.5	0.00834	0.09877	0.00007	0.11500	5.42×10^{-4}
18.0	0.00803	0.09668	0.00007	0.10682	5.54×10^{-4}
18.5	0.00819	0.09460	0.00006	0.12885	8.87×10^{-4}
19.0	0.00858	0.09058	0.00005	0.10799	5.73×10^{-4}
19.5	0.00886	0.08791	0.00004	0.09361	4.68×10^{-4}
20.0	0.00921	0.08543	0.00003	0.07084	3.85×10^{-4}
20.5	0.00937	0.08243	0.00003	0.07158	6.12×10^{-4}
21.0	0.01438	0.08260	0.00003	0.06546	5.90×10^{-4}

The magnetic data of compound 7*R*.

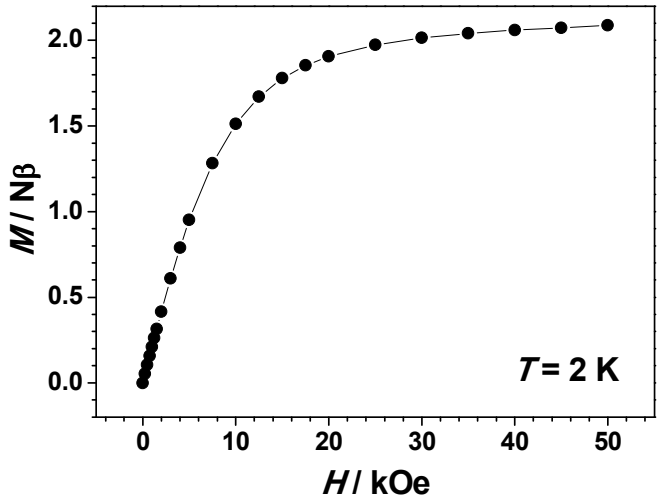

Figure S56. Isothermal magnetization for **7*R*** from 0 T to 5 T at 2.0 K.

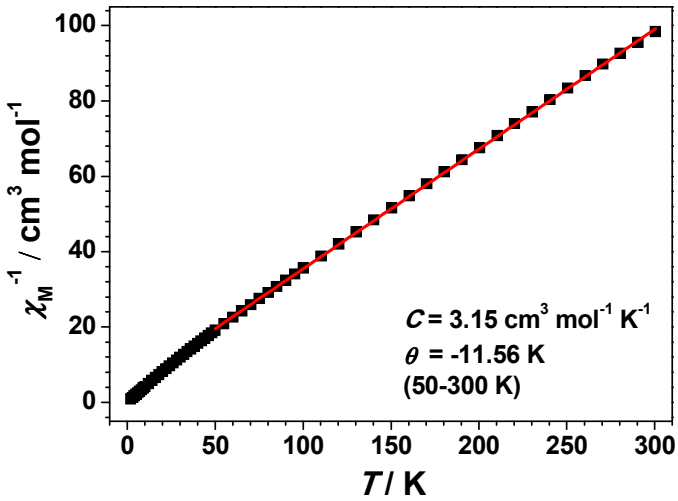

Figure S57. Plots of χ_M^{-1} *vs*. *T* for **7*R*** under 1 kOe dc field (The red solid line represents the best fit to the Curie-Weiss expression).

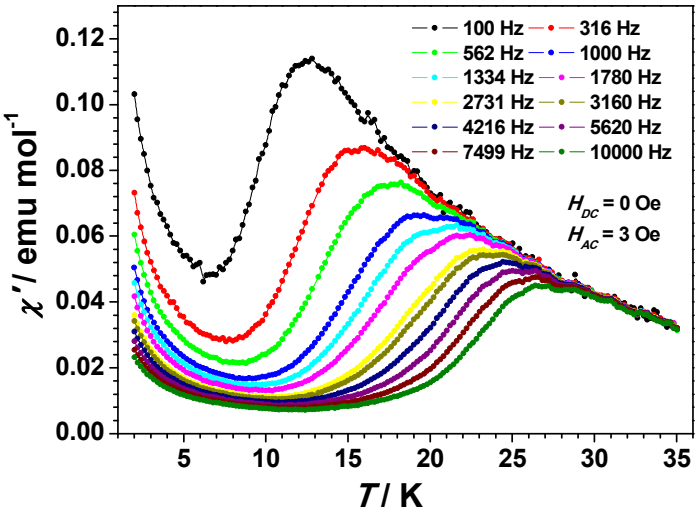

Figure S58. Temperature dependence of χ' (in-phase) of **7*R*** in the absence of dc field range from 2.0 K to 35.0 K in PPMS.

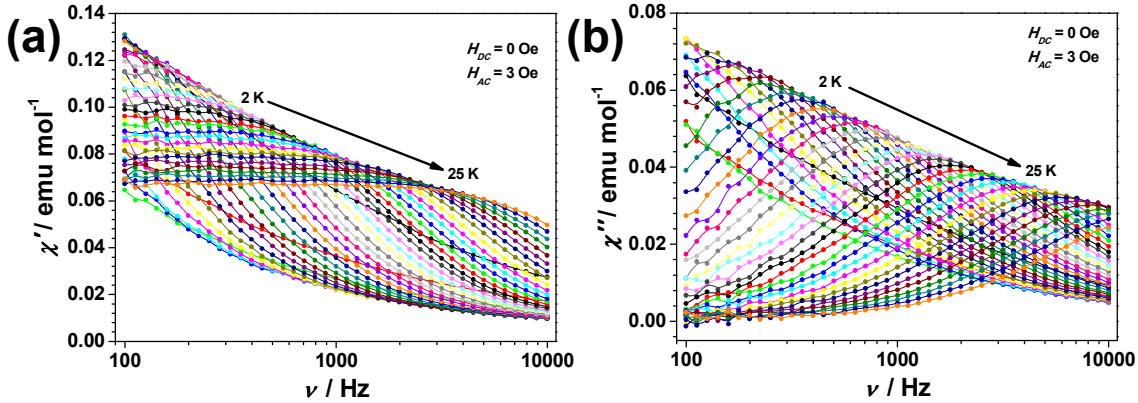

Figure S59. Frequency dependence (100-10000 Hz) of ac susceptibility (a) in-phase and (b) out-of-phase of **7*R*** in the absence of dc field range from 100 to 10000 Hz at different temperatures (2 K to 8 K, 2 K interval, 8.5 K to 25 K, 0.5 K interval) in PPMS.

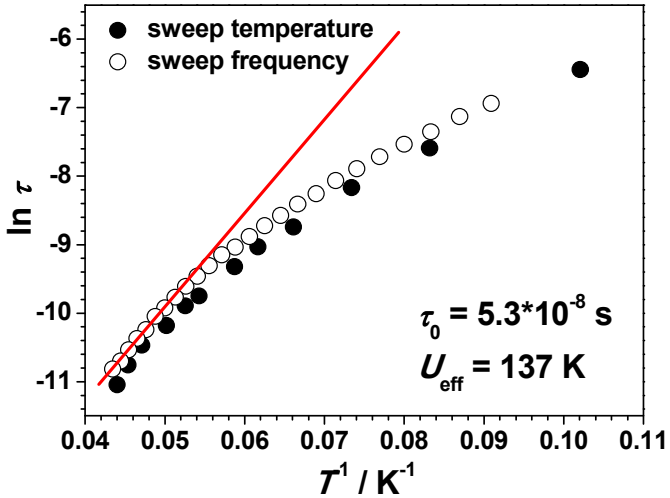

Figure S60. Arrhenius plots of relaxation times of **7*R*** in the absence of dc field, the data was collected from the peaks of χ'' (out-of-phase) against temperature and the peaks of χ'' (out-of-phase) against frequency at different temperatures.

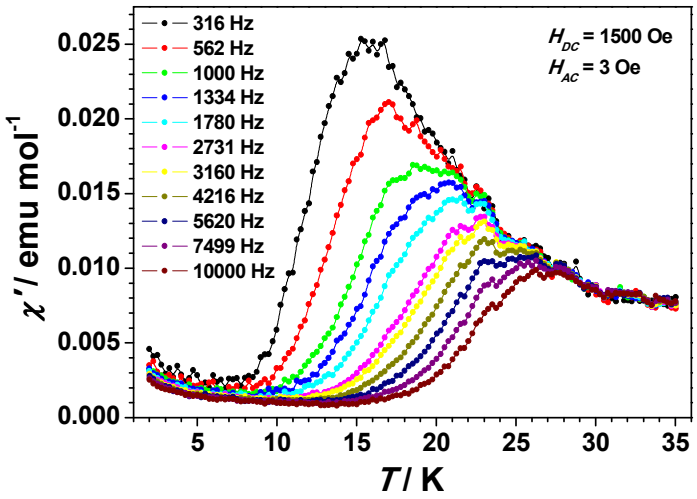

Figure S61. Temperature dependence of χ' (in-phase) of **7*R*** under a dc field of 1500 Oe range from 2.0 K to 35.0 K in PPMS.

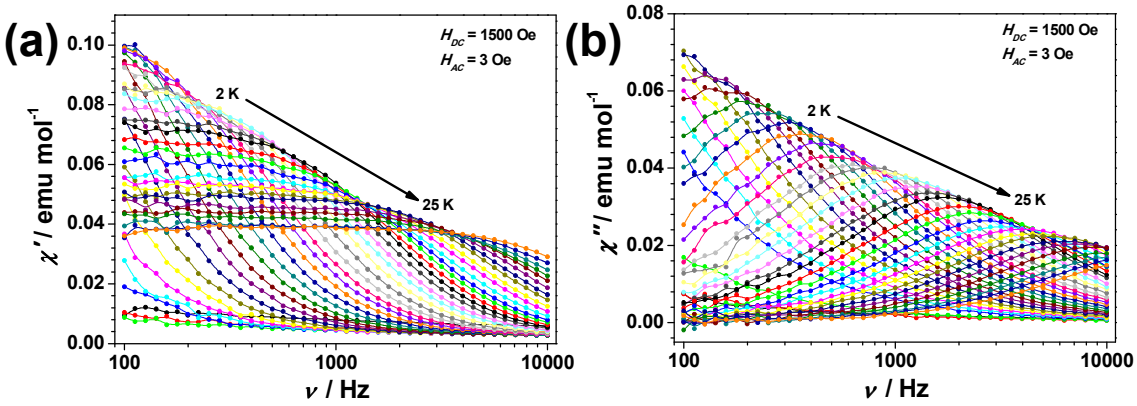

Figure S62. Frequency dependence (100-10000 Hz) of ac susceptibility (a) in-phase and (b) out-of-phase of **7*R*** under a dc field of 1500 Oe range from 100 to 10000 Hz at different temperatures (2 K to 8 K, 2 K interval, 8.5 K to 25 K, 0.5 K interval) in PPMS.

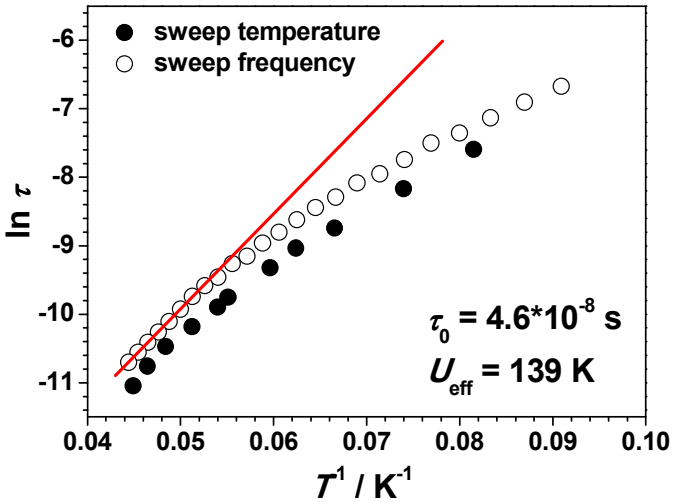

Figure S63. Arrhenius plots of relaxation times of **7*R*** under a dc field of 1500 Oe, the data was collected from the peaks of χ'' (out-of-phase) against temperature and the peaks of χ'' (out-of-phase) against frequency at different temperatures.

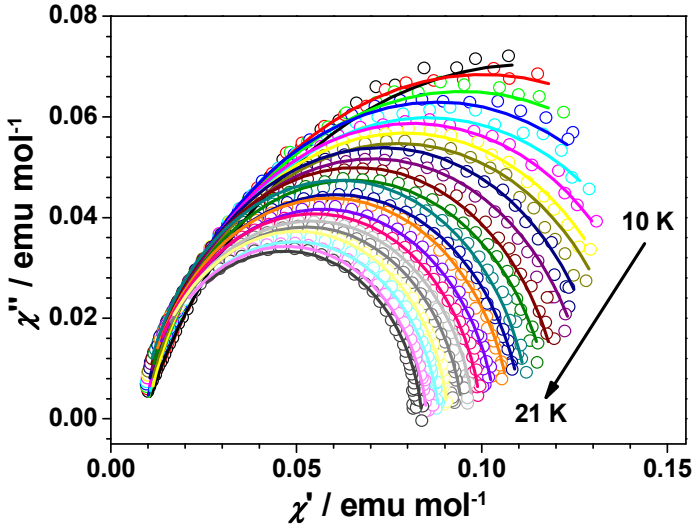

Figure S64. Cole-Cole diagram of **7*R*** in the absence of dc field from 10 K to 21 K (ac frequencies from 100 Hz to 10000 Hz, 0.5 K interval).

Table S14. The parameters of Cole-Cole fitting of **7*R*** in the absence of dc field.

T (K)	X_0	X_t	τ (s)	α	R
10.0	0.00862	0.20354	0.00171	0.20343	1.38×10^{-3}
10.5	0.00874	0.18346	0.00117	0.15410	1.22×10^{-3}
11.0	0.00875	0.17334	0.00104	0.14807	2.17×10^{-3}
11.5	0.00881	0.16163	0.00080	0.12257	1.98×10^{-3}
12.0	0.00894	0.15623	0.00065	0.13116	8.28×10^{-4}
12.5	0.00867	0.14957	0.00050	0.11569	6.10×10^{-4}
13.0	0.00967	0.14444	0.00046	0.10833	1.00×10^{-3}
13.5	0.00859	0.14161	0.00036	0.12362	9.54×10^{-4}
14.0	0.00850	0.13409	0.00032	0.09678	8.77×10^{-4}
14.5	0.00832	0.12954	0.00025	0.10067	6.07×10^{-4}
15.0	0.00832	0.12176	0.00019	0.08078	1.25×10^{-3}
15.5	0.00831	0.11895	0.00019	0.09728	6.39×10^{-4}
16.0	0.00829	0.11304	0.00015	0.06315	3.97×10^{-4}
16.5	0.00832	0.11099	0.00013	0.08957	6.85×10^{-4}
17.0	0.00834	0.10797	0.00012	0.08105	5.36×10^{-4}
17.5	0.00834	0.10393	0.00011	0.08733	5.00×10^{-4}
18.0	0.00843	0.09997	0.00009	0.07327	6.61×10^{-4}
18.5	0.00845	0.09796	0.00007	0.08200	4.63×10^{-4}
19.0	0.00861	0.09494	0.00007	0.07890	6.34×10^{-4}
19.5	0.00865	0.09092	0.00006	0.06273	4.92×10^{-4}
20.0	0.00847	0.08856	0.00005	0.08213	3.30×10^{-4}
20.5	0.00853	0.08519	0.00004	0.07115	3.80×10^{-4}
21.0	0.00847	0.08393	0.00003	0.07890	4.22×10^{-4}

The magnetic data of compound 8*R*.

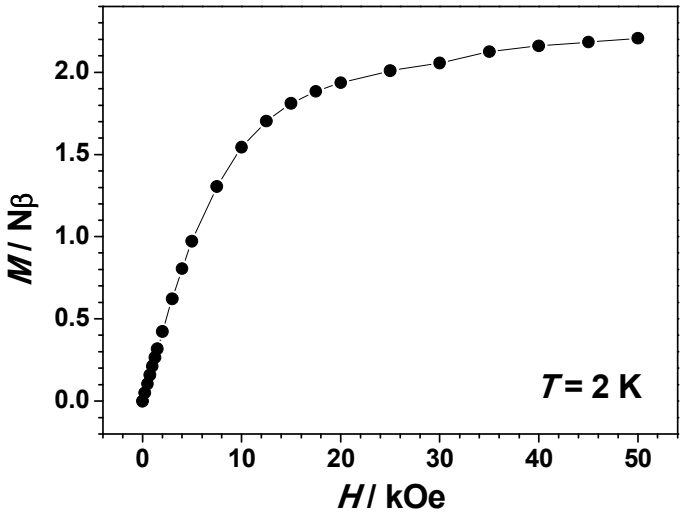

Figure S65. Isothermal magnetization for **8*R*** from 0 T to 5 T at 2.0 K.

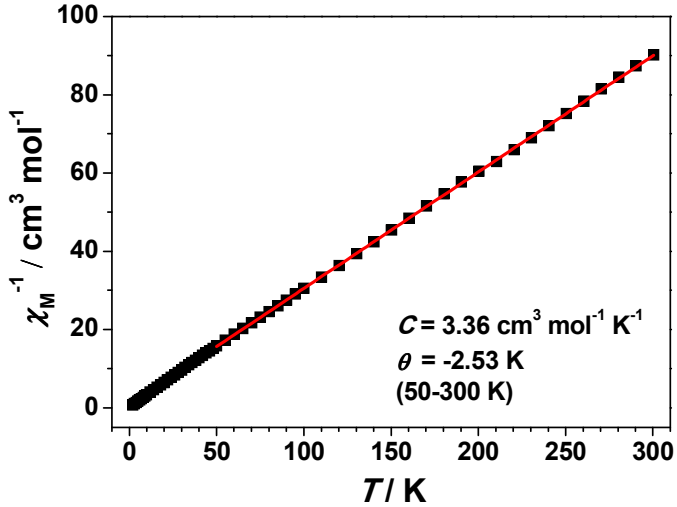

Figure S66. Plots of χ_M^{-1} *vs*. *T* for **8*R*** under 1 kOe dc field (The red solid line represents the best fit to the Curie-Weiss expression).

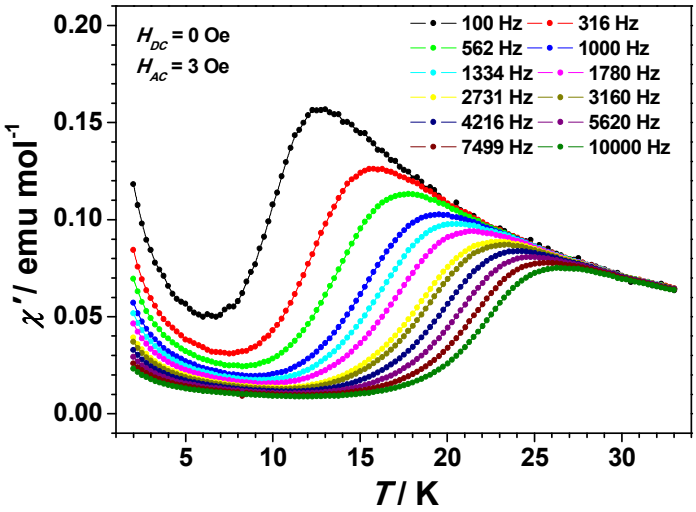

Figure S67. Temperature dependence of χ' (in-phase) of **8*R*** in the absence of dc field range from 2.0 K to 33.0 K in PPMS.

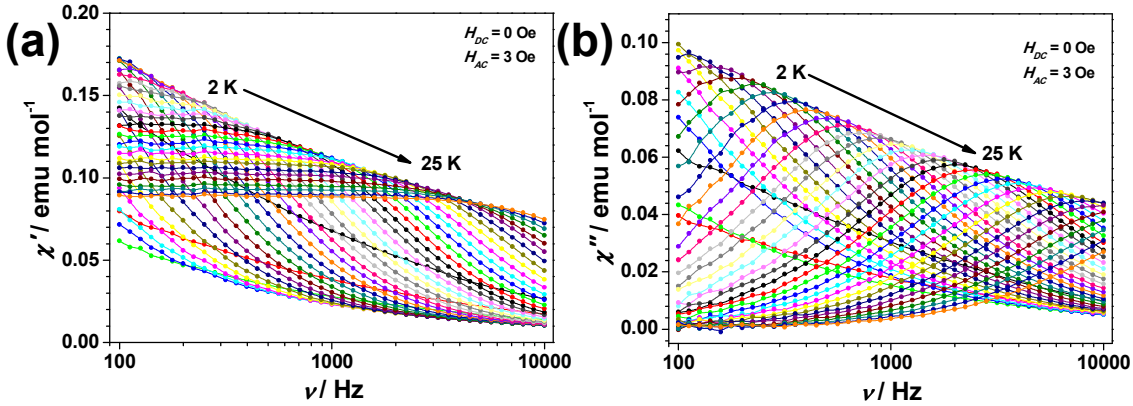

Figure S68. Frequency dependence (100-10000 Hz) of ac susceptibility (a) in-phase and (b) out-of-phase of **8*R*** in the absence of dc field range from 100 to 10000 Hz at different temperatures (2 K to 8 K, 2 K interval, 8.5 K to 25 K, 0.5 K interval) in PPMS.

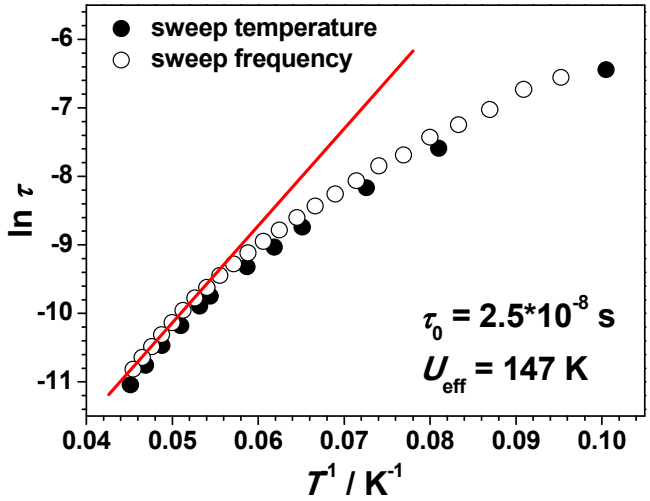

Figure S69. Arrhenius plots of relaxation times of **8*R*** in the absence of dc field, the data was collected from the peaks of χ'' (out-of-phase) against temperature and the peaks of χ'' (out-of-phase) against frequency at different temperatures.

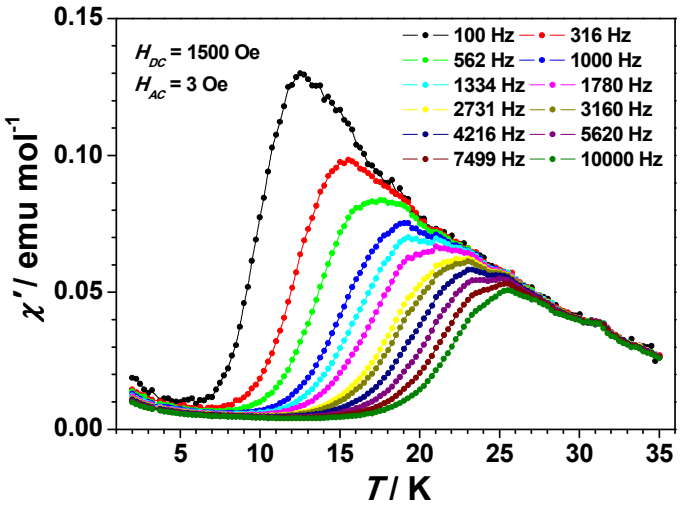

Figure S70. Temperature dependence of χ' (in-phase) of **8*R*** under a dc field of 1500 Oe range from 2.0 K to 35.0 K in PPMS.

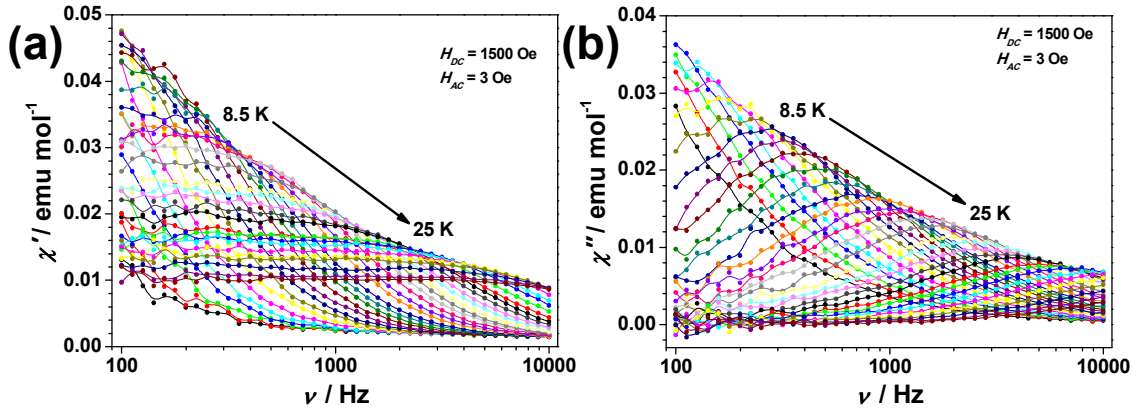

Figure S71. Frequency dependence (100-10000 Hz) of ac susceptibility (a) in-phase and (b) out-of-phase of **8*R*** under a dc field of 1500 Oe at different temperatures (8.5 K to 25 K, 0.5 K interval) in PPMS.

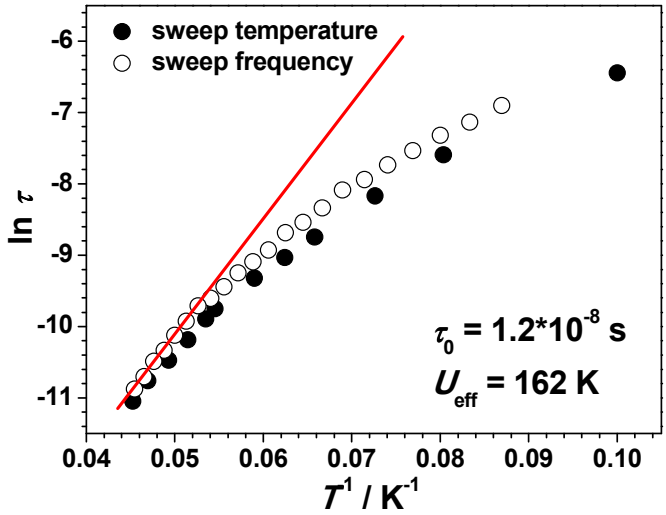

Figure S72. Arrhenius plots of relaxation times of **8*R*** under a dc field of 1500 Oe, the data was collected from the peaks of χ'' (out-of-phase) against temperature and the peaks of χ'' (out-of-phase) against frequency at different temperatures.

Table S15. The parameters of Cole-Cole fitting of **8*R*** in the absence of dc field.

T (K)	X_0	X_t	τ (s)	α	R
9.0	0.01073	0.25688	0.00281	0.15719	5.39×10^{-3}
9.5	0.01086	0.28244	0.00275	0.17087	2.59×10^{-3}
10.0	0.01083	0.26219	0.00197	0.15436	1.39×10^{-3}
10.5	0.01077	0.24307	0.00138	0.13268	1.14×10^{-3}
11.0	0.01080	0.23153	0.00111	0.11595	1.04×10^{-3}
11.5	0.01080	0.22654	0.00093	0.13197	6.71×10^{-4}
12.0	0.01079	0.21665	0.00071	0.12875	6.45×10^{-4}
12.5	0.01070	0.20252	0.00057	0.09889	5.56×10^{-4}
13.0	0.01081	0.19173	0.00042	0.08287	7.56×10^{-4}
13.5	0.01174	0.18390	0.00036	0.07142	5.73×10^{-4}
14.0	0.00939	0.17790	0.00030	0.07710	3.85×10^{-4}
14.5	0.01043	0.16829	0.00024	0.05323	4.88×10^{-4}
15.0	0.01057	0.16278	0.00021	0.07119	4.31×10^{-4}
15.5	0.00964	0.15735	0.00017	0.06476	3.33×10^{-4}
16.0	0.00946	0.15301	0.00014	0.07218	6.57×10^{-4}
16.5	0.00857	0.14694	0.00013	0.05711	3.38×10^{-4}
17.0	0.00858	0.14275	0.00010	0.06867	5.10×10^{-4}
17.5	0.00826	0.13851	0.00009	0.05042	2.59×10^{-4}
18.0	0.00782	0.13453	0.00008	0.06560	4.22×10^{-4}
18.5	0.00803	0.13131	0.00006	0.06874	3.37×10^{-4}
19.0	0.00863	0.12826	0.00006	0.07247	4.22×10^{-4}
19.5	0.00824	0.12412	0.00005	0.08021	3.29×10^{-4}
20.0	0.00771	0.11924	0.00004	0.06961	3.01×10^{-4}
20.5	0.00769	0.11720	0.00004	0.07918	6.58×10^{-4}
21.0	0.00878	0.11242	0.00003	0.04548	8.33×10^{-4}

Theoretical calculation data

Table S16. Calculated spin-free energies (cm^{-1}) of the lowest terms of the central Co(II) fragment of compounds **1**–**8**.

Spin mult.	**1*R***	**2*R***	**3*R***	**4*R***	**5*R***	**6*R***	**7*R***	**8*R***
4	0.0	0.0	0.0	0.0	0.0	0.0	0.0	0.0
4	95.1	1665.4	1532.3	1849.1	86.2	127.7	107.7	265.4
4	12588.3	7809.6	6813.4	7648.2	12298.9	12107.9	12857.9	12535.6
4	12776.1	15690.8	16820.2	14834.8	12674.6	13078.0	13094.7	13022.0
4	48820.1	50156.6	56712.3	48350.2	49273.8	49242.8	41432.3	49684.8
4	49709.5	51196.9	57813.2	49279.6	50147.5	49982.2	44207.6	50487.4
4	50308.4	52079.2	58123.8	50921.7	50619.3	50672.7	44505.0	51214.1
4	52346.6	53593.6	59461.2	52904.3	52518.4	52858.8	48599.1	53370.9
4	56040.6	57815.4	61423.8	55195.8	56143.3	56078.6	51215.8	56607.2
4	56933.6	58931.7	62421.9	56116.0	57061.1	56877.7	51267.9	57368.2
2	16114.3	14652.9	15793.0	14988.2	16145.6	15237.9	16245.6	16663.7
2	17882.6	17018.2	19219.7	16573.4	18025.2	18015.6	18619.6	17924.2

Table S17. Calculated energies (cm^{-1}) of the lowest Kramers doublets of compounds **1**–**8**.

1*R*	**2*R***	**3*R***	**4*R***	**5*R***	**6*R***	**7*R***	**8*R***
0.0	0.0	0.0	0.0	0.0	0.0	0.0	0.0
305.7	69.4	81.6	60.0	306.5	302.0	294.3	280.9
645.1	1758.5	1812.3	1931.4	643.5	650.9	626.4	699.8
978.3	1861.7	1971.2	2017.8	977.6	980.2	945.8	1007.4
12851.9	7905.9	8005.6	7744.1	12616.3	12471.1	13121.2	12797.7
12975.5	7932.5	8078.4	7766.4	12708.3	12510.9	13235.0	12876.9

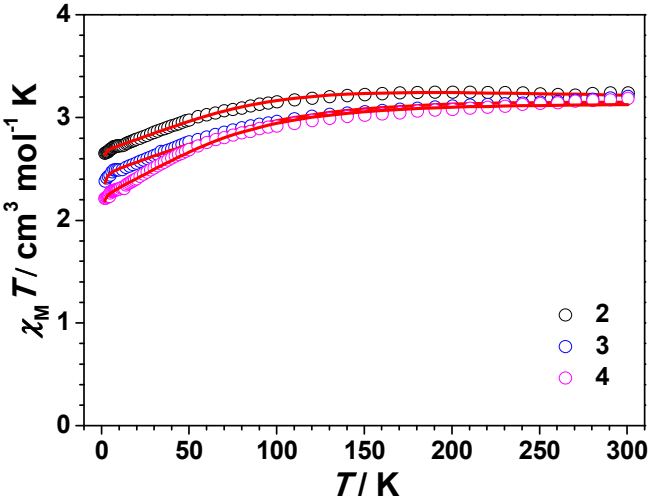

Figure S73. Experimental and fitting $\chi_M T$ *vs.* T plots of **2**, **3**, and **4** at 2–300 K, red solid line indicate the best fits with PHI program.

Circular dichroism (CD) spectrum

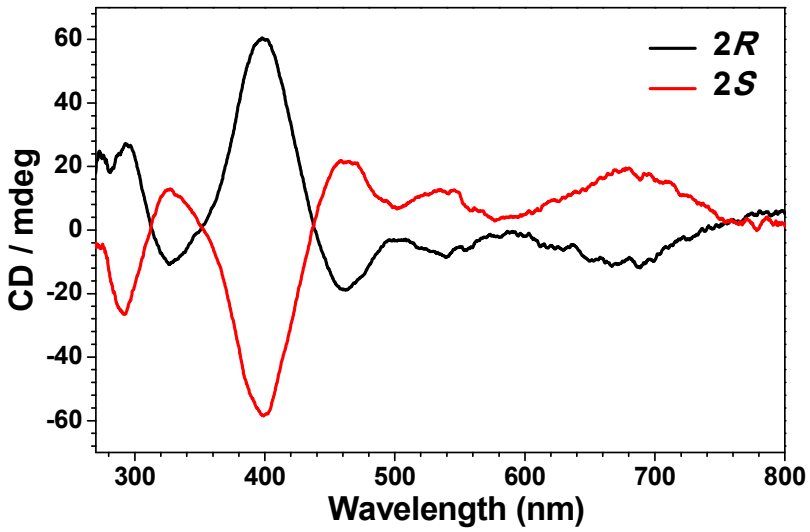

Figure S74. The solid-state CD spectra of **2*R*** (black) and **2*S*** (red) in KBr pellet at 298 K.